doi:10.20944/preprints202104.0623.v1

Towards clean and safe water: a review on the emerging role of imprinted polymer-based electrochemical sensors

Xiaofeng Zheng[1], Sohayb Khaoulani[2], Nadia Ktari[3], Momath Lo[4], Ahmed M. Khalil[5,6],
Chouki Zerrouki[2], Najla Fourati[2,*], Mohamed M. Chehimi[1,6*]

[1] Université de Paris, CNRS, ITODYS (UMR 7086), 75013 Paris, France;
xiao-feng.zheng@etu.u-paris.fr (X. Z.); mmchehimi@yahoo.fr (M. M. C.)
[2] SATIE, UMR CNRS 8029, Cnam, 75003 Paris, France ; sohayb.khaoulani@lecnam.net (S. K.),
najla.fouratiennouri@lecnam.net (N.F.) ; chouki.zerrouki@lecnam.net (C.Z.)
[3] Laboratoire Matériaux, Traitement et Analyse, INRAP, BiotechPole Sidi-Thabet, 2032, Ariana,
Tunisia ; ktarinadia@gmail.com (N. K.)
[4] Université Cheikh Anta Diop, Faculté des Sciences, Département de Chimie,
Laboratoire de Chimie Physique Organique & Analyse Instrumentale, Dakar, Senegal ;
momath.lo@ucad.edu.sn (M. L.)
[5] Photochemistry Department, National Research Centre, Dokki, 12622 Giza, Egypt;
akhalil75@yahoo.com (A. M. K.)
[6] Université Paris Est, ICMPE (UMR7182), CNRS, UPEC, F-94320 Thiais, France

Corresponding author: Mohamed M. Chehimi, Université de Paris, ITODYS, UMR 7086, CNRS,
F-75013 Paris, France ; mmchehimi@yahoo.fr , ORCID: 0000-0002-6098-983X

Keywords: imprinted polymers; electrochemical sensors; pesticides; metal ions; bacteria.

Abstract

This mini-review critically summarizes the knowledge of imprinted polymer-based electrochemical sensors, for the detection of pesticides, metal ions and waterborne pathogenic bacteria, focusing on the period the last 5 years (citation of 78 papers published in 2017-2021, *ie* 63% of total citations). MIP-based electrochemical sensors exhibit low limit of detection, high selectivity, high sensitivity and low cost. Herein, we focused on the timely topics of water pollution by organics, inorganics and micro-organisms represented by pesticides, metal ions and bacteria, respectively. We put the emphasis on the design of imprinted polymers and their composites and coatings by radical polymerization, oxidative polymerization of conjugated monomers or sol-gel chemistry. Whilst most imprinted polymers are used in conjunction with differential pulse or square wave voltammetry for sensing organics and metal ions, electrochemical impedance spectroscopy (EIS) appears as the chief technique for detecting bacteria. This successful combination of EIS and imprinting technology should be harnessed in the coming years in the case of bacteria. Interestingly, bacteria are not always probed by bacteria-imprinted polymers; we report here their detection by monitoring specific (macro)molecules that reflect bacterial activity, for example quorum sensing signaling molecules or flagella proteins. If much has been developed in the past decade with glassy carbon or gold electrodes, it is clear that carbon paste electrodes of imprinted polymers are more and more investigated due to their versatility. Shortlisted case studies were critically reviewed and discussed; clearly a plethora of tricky strategies of designing selective electrochemical sensors are offered to “Imprinters”. We anticipate this review will be of interest to experts and new comers in the field who are paying time and effort combining electrochemical sensors with MIP technology.

1. Introduction

Human activities revolve around water, be it in industry, chemistry, agriculture or even for living. Therefore, it is unavoidable that water ends up polluted [1]. Water pollution refers to all substances that human activity introduces into water, be it toxic or benign pollutants.

Water depollution is a major issue nowadays, however in order to eliminate harmful substances, one needs to first characterize and quantify them in order to design appropriate pollutant removal methods, e.g. by adsorption, filtration or degradation. In this sense, the detection of species needs to be accurate and selective. Several methods meet these requirements, but they often require expensive materials and instruments; moreover the measurement time is a significant criterion.

Towards this end, electrochemistry is an excellent means of sensing pollutants because of its high sensitivity (it goes down to femtomolar), selectivity and low cost [2]. Furthermore, the measurements are easy to set up and above all miniaturization is possible so that electrosensing measurements could be directly taken near water sources using portable devices [3].

Sensitivity is certainly an important characteristic of sensors and could even be more decisive parameter. In this regard, bio-inspired molecularly imprinting polymer (MIP) stand as excellent sensing materials. They can be prepared in bulk or as thin layers on the electrode surface, could have high sensitivity by nanostructuration and last but not least they are selective by design. Indeed, MIPs are prepared in the crosslinked form in the presence of a template species (organics, metal ion, microorganism) which leave receptor sites in the polymer network upon removal by appropriate solvents. The receptor sites recognize the template at the rebinding step with excellent selectivity. Moreover, the low cost design of MIPs and easiness. Electrochemical sensors using MIP as the selective layer are increasingly studied in various domains: in medicine to detect and capture biologic molecules [4], in food industry for quality control and food security [5, 6], or to track heavy metal ions to monitor water quality [7]. Moreover, advances on transducers, for example carbon based nanostructured materials, enable the increase in performance of MIPs [8].

2. Scope of the review

This review summarizes applications of MIP based electrochemical sensor in the detection of pollutants in water sources. Pollutants are divided into 3 categories: organic molecules, metal ions and pathogens. Several reviews were devoted to the electrochemical detection of such pollutants as reported in Table 1. However, they are either too general or target selected series of compounds or ions.

Table 1. Handpicked reviews on MIPs for the detection of chemicals and pathogenic microoragnisms**.**

Running title	**Scope of review**	**Year of publication**	**Refs.**
Recent advances on IIP	Overview of general method of preparation of ion-imprinted polymers	2013	[9]
Monitoring of metals using IIP	Overview of IIP fabrication and applications in different domains.	2015	[10]
MIP for electrochemical detection of drugs	This paper critically reviews applications of MIP-based electrochemical sensors for the detection of drugs.	2018	[11]
MIP-based sensor for detection of food hazard	General overview of MIP-based optical, electrochemical and gravimetric sensors of hazardous compounds in food.	2019	[5]
Electrochemical sensors based on MIP and nanomaterials	Recent advances on MIP- and nanomaterial-based electrochemical sensors, without specific targets.	2019	[12]
Overview of recent nanostructured MIP based sensors for pesticide detection	A study on existing NP-MIP based sensors for pesticide, showing their fabrication method and experimental result.	2020	[13]
Applications of chitosan in molecularly and ion imprinted polymers	A brief overview of recent applications of chitosan-based MIPs and MIP composites.	2020	[14]

We have surveyed the recent progress in the design and applications of MIP-based electrochemical sensors of pesticides, metal ions and pathogenic bacteria. We emphasize the last five years: we cited 78 papers published in 2017-2021, *ie* 63% of total citations.

The review is organized as follows:

- Methods of synthesis of molecularly imprinted polymers
- Design of sensing electrodes
- Electrochemical characterization techniques
- Case studies of applications of imprinted polymer-based electrochemical sensors to pesticides, heavy metal ions and bacteria.

The case studies will be split in three main sub-sections and will concern pesticides, metal ions and bacteria. Each case study section, devoted to a given pollutant, will describe either imprinted vinylic, conjugated or sol-gel polymeric materials prepared in thin films or as finely divided nanocomposite powders. Besides these polymers, there is growing interest in employing imprinted chitosan-based adsorbents in electrochemical sensors; the reader is referred to recent reviews and original articles [14-16].

3. Methods of preparation of imprinted polymers and electrode materials

3.1. Monomers and polymers

MIPs are synthetized by (co-)polymerization of functional monomers and cross-linkers in the presence of template compounds or microorganism (Figure 1a). Chelators could be added in the pre-polymerization mixture, in a variety of solvents [17, 18]. After synthesis, templates are removed from the crosslinked polymeric matrix or coating, leaving three-dimensional cavities which are complementary in terms of shape and functional groups to the targeted compound or microorganism. Figure 1b illustrates well the concept of molecular imprinting with a picture of a slice of cake cooked with candied fruits. Clearly, the candied fruits leave prints in the cake once removed and the shape fit in well only with the ingredient ("template") used to cook the cake and that has been removed. Parts of the cake slice that has no candied fruit corresponds to the non-imprinted polymer. At the molecular level, shape only does not suffice to have a good sensor; interfacial interactions highly matter and this is the reason for using functional monomers that tightly bind the template molecules. MIPs were widely used as solid phase extractors and as sensitive recognition elements of chemical and biological sensors [19-21].

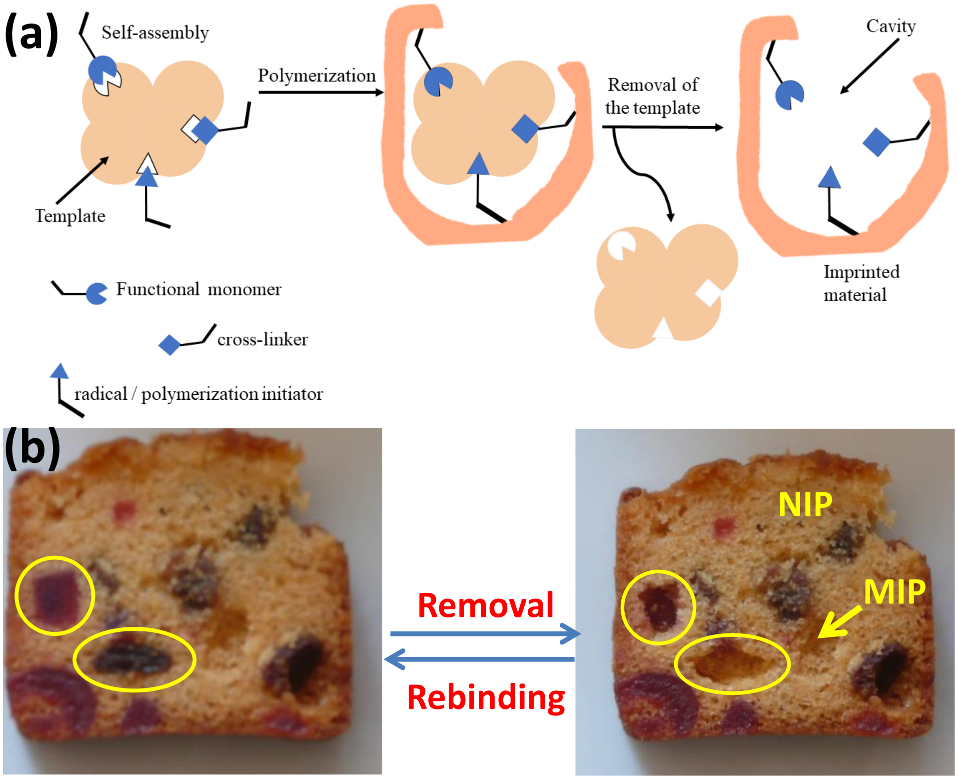

Figure 1. Principle of making MIPs (a), and illustration of the imprinting technique by digital photographs of a slice of cake before after removal of candied fruits (b).

Imprinted organic and sol-gel polymers can be prepared using a large variety of monomers, the choice depending on the application (Table 2).

Table 2. Selected, commercially available monomers frequently employed for making MIPs. Pyrrole is displayed with its corresponding 2D microstructure.

Functional monomers	Crosslinkers
Vinylic monomers	
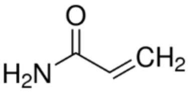 Acrylamide 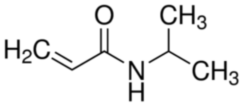 *N*-Isopropylacrylamide 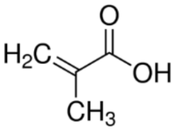 Methacrylic acid 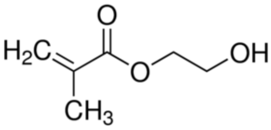 2-Hydroxyethyl methacrylate 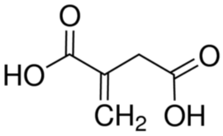 Itaconic acid 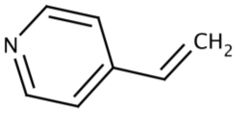 4-Vinylpyridine 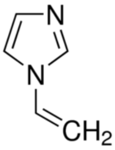 1-Vinylimidazole	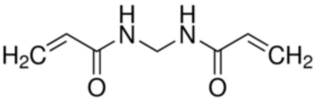 *N,N'*-(1,2-Dihydroxyethylene)bisacrylamide 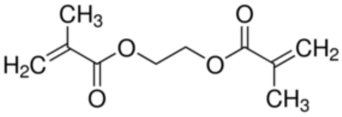 Ethylene glycol dimethacrylate 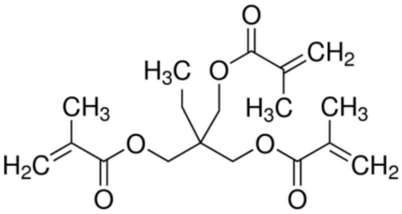 Trimethylolpropane trimethacrylate 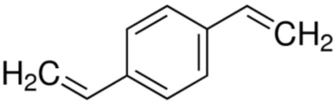 *p*-Divinylbenzene
Conjugated monomers	
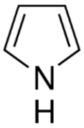 Pyrrole 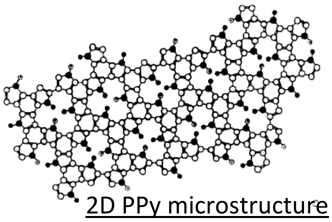 2D PPy microstructure	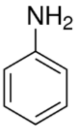 Aniline 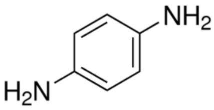 *p*-Phenylenediamine
Silanes	
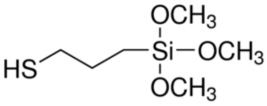 (3-Mercaptopropyl) trimethoxysilane 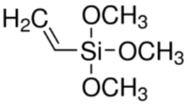 Vinyltrimethoxysilane 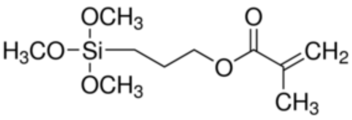 3-(Trimethoxysilyl)propyl methacrylate	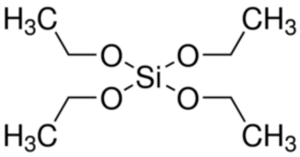 Tetraethyl orthosilicate

Most of the studies concern the preparation of crosslinked vinylic polymers or conjugated polymers such as polypyrrole and polyaniline. It is important to note, that the latter do not require crosslinking monomers as they are well-known to have rigid 3D structure and polypyrrole is even naturally crosslinked ([22], [23]). Besides organic monomers, there are several reports on imprinted sol-gel inorganic polymers based on silica. As a matter of fact, we would like to recall here that the very first imprinted polymers were designed by Dickey [24] (Figure 2) and concerned alkyl orange dye-imprinted silicas prepared by sol-gel chemistry. It was demonstrated that the adsorbent was selective for the uptake of the dye used in the preparation of the gel. Hence, preparation of gel using methyl orange led to selective adsorption of this dye over ethyl, propyl and butyl orange dyes. Similar trends were obtained for the three other syntheses. The organic imprinted polymers were introduced in the 1972s by Wulff and Sahran [25] to describe the concept of “enzyme-analogue built polymers”, that is decades after Dickey’s work.

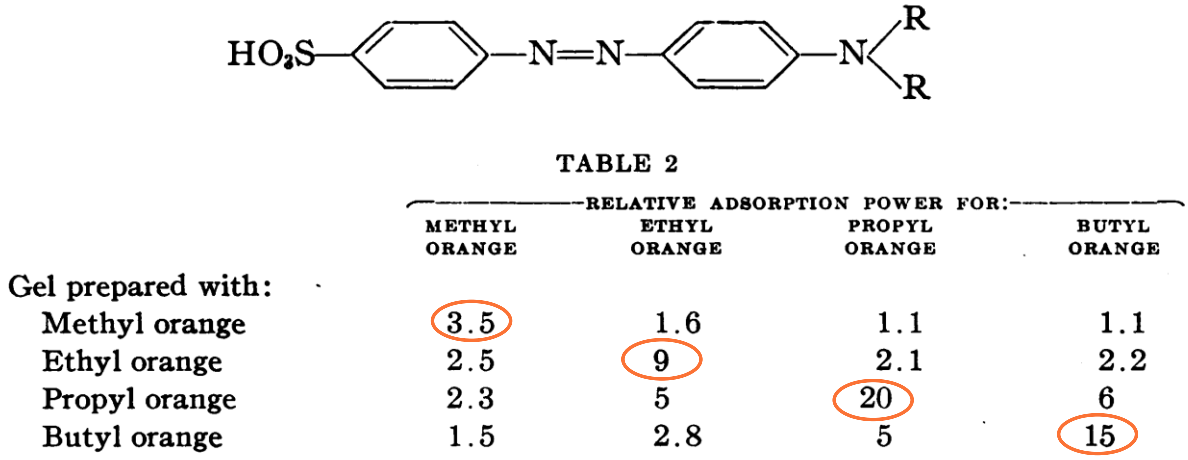

TABLE 2

	RELATIVE ADSORPTION POWER FOR:			
	METHYL ORANGE	ETHYL ORANGE	PROPYL ORANGE	BUTYL ORANGE
Gel prepared with:				
Methyl orange	3.5	1.6	1.1	1.1
Ethyl orange	2.5	9	2.1	2.2
Propyl orange	2.3	5	20	6
Butyl orange	1.5	2.8	5	15

Figure 2. Screenshot of Dickey’s paper: Chemical structure of methyl orange and results of its relative adsorption (Adapted from [24]).

3.1.1. Vinylic imprinted polymers

Most of imprinted vinylic polymer powders, nanocomposites and coatings are prepared via free radical polymerization using AIBN, Irgacure or potassium persulfate. Free radical or photoinduced radical polymerization or controlled photopolymerization (such as photo-iniferter [26, 27], INItiation – TransFER – TERminaison agent) is ideal as it does not require heating and could be achieved within minutes-to-a few hours. In the case of grafted imprinted polymers, photopolymerization is unique for its spatiotemporal aspect. The polymer can be grafted on a selected area and growth be controlled with irradiation time. Ion imprinted clay-polymer nanocomposites have recently been prepared by radical photopolymerization under visible [28] or UV light [29] using Type II photoinitiators. For surface confined MIP grafted thin films prepared by photopolymerization, the reader is referred to [30, 31].

Figure 3 shows simplified mechanism of radical polymerization whether it is of the free radical or controlled type. Initiator is activated thermally or photochemically and the initiating radical triggers polymerization of the PCC to yield after a few hours or better a few minutes (in the case of photopolymerization), 3D crosslinked polymers with entrapped template species (T). Precipitation polymerization requires crashing of the former monolith; but in the case of thin film imprinted polymer synthesis, it is essential to first prepare electrode grafted with initiators in order to confine polymerization to the surface and limit precipitation of imprinted polymers or interpenetration of grafted polymers with free crosslinked polymer; this makes cleaning the grafted imprinted polymer tedious. For example, Type II radical photoinitiators are preferred over Type I phtoinitiators as they drastically limit bulk solution polymerization. Type I photoinitiators give two radicals upon thermal or photo-clevage: initiating radicals in solution and at the surface.

As far as electrochemical sensors are concerned, a great deal of studies concerned the nanostructuration of vinylic imprinted polymers by metallic or carbon nanoparticles [32, 33] which can be coated on free electrode surfaces or mixed with graphite in order to prepare carbon paste electrodes. Such nanostructuration enhances the conductivity of the polymer and facilitates electron transfer.

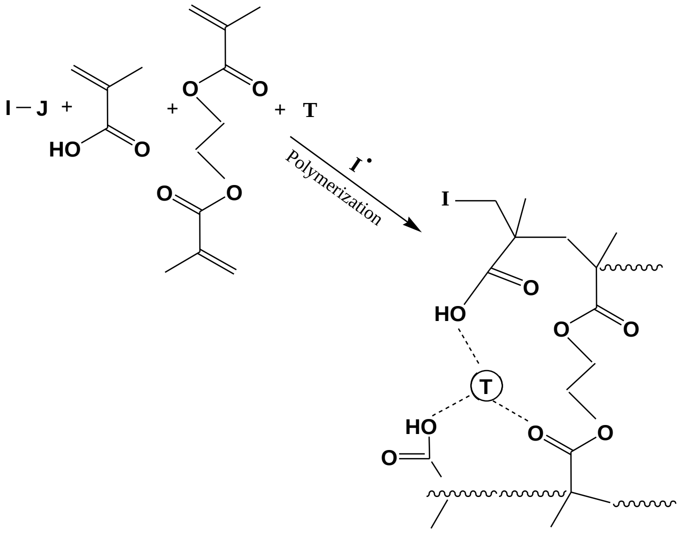

Figure 3. Simplified mechanism of imprinted vinylic polymer synthesis by radical polymerization. Example is given for methacrylic acid functional monomer and EGDMA crosslinker. I-J is the initiator and T the template.

3.1.2. Conductive polymers

Conducting polymers (CPs) are π-conjugated organic materials with electrical and optical properties comparable to those of inorganic semiconductors and metals. They can be synthesized using cost-effective, simple and versatile approaches. Several methodologies have been developed to prepare CPs (precipitation polymerization, electropolymerization, sonochemical synthesis and photopolymerization). Electropolymerization remains, however, the most investigated technique as it permits to address the morphology, thickness and conductivity of CPs and is suitable for electrochemical sensors [34]. These features led to increased application of CPs in the fabrication of chip-based sensors, biosensors, diagnostic and environmental monitoring devices [35-38]. However, with the development of conductive polymer nanocomposites, oxidative chemical polymerization of conjugated monomers is versatile because the same nanocomposites could be employed as adsorbents or mixed with graphite powder to make carbon paste electrodes for selective electrochemical sensors. If chemical method could require one or two hours, electropolymerization is most probably the fastest process among all other discussed in this review. Moreover, electropolymerization is conducted in aqueous media in a supporting electrolyte with or without ligand if IIP is meant to be prepared.

Figure 4 depicts general pathways for polypyrrole and polyaniline syntheses. Bearing N-H groups, these polymers have the ability to interact with the template in the course of the polymerization process.

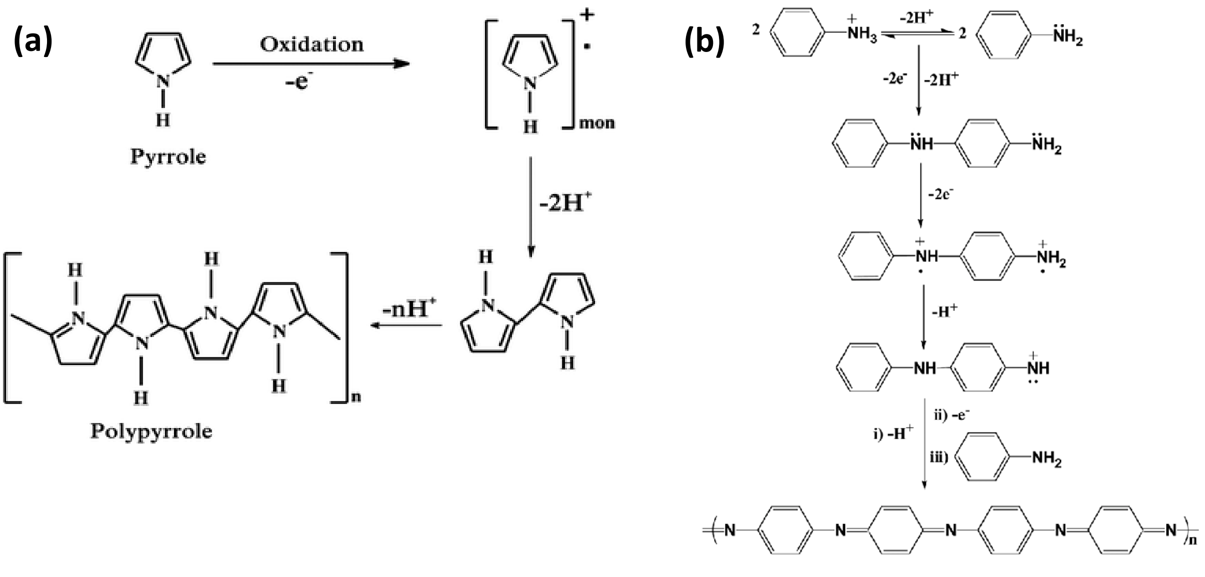

Figure 4. Simple pathways for the synthesis of polypyrrole (a) and polyaniline (b). Reproduced from [39].

3.1.3. Sol-gel synthesis

Sol-gel process has been intensively used for the synthesis of porous nanostructures mainly composed of transition metal alkoxides and siloxane (Si−O) backbone structure [40]. Three reactions steps are generally involved during a given sol-gel procedure: *(i)* interaction between metal cation and water molecules, *(ii)* hydrolysis of silicone monomers, and *(iii)* polycondensation of the silica into a porous-3D network. Sol-gel chemistry provides a relatively simple way for the design of materials and composites, which can be used as functionalization layers of electrochemical sensing devices [41-43]. A schematic representation of sol-gel methods is depicted in Figure 5.

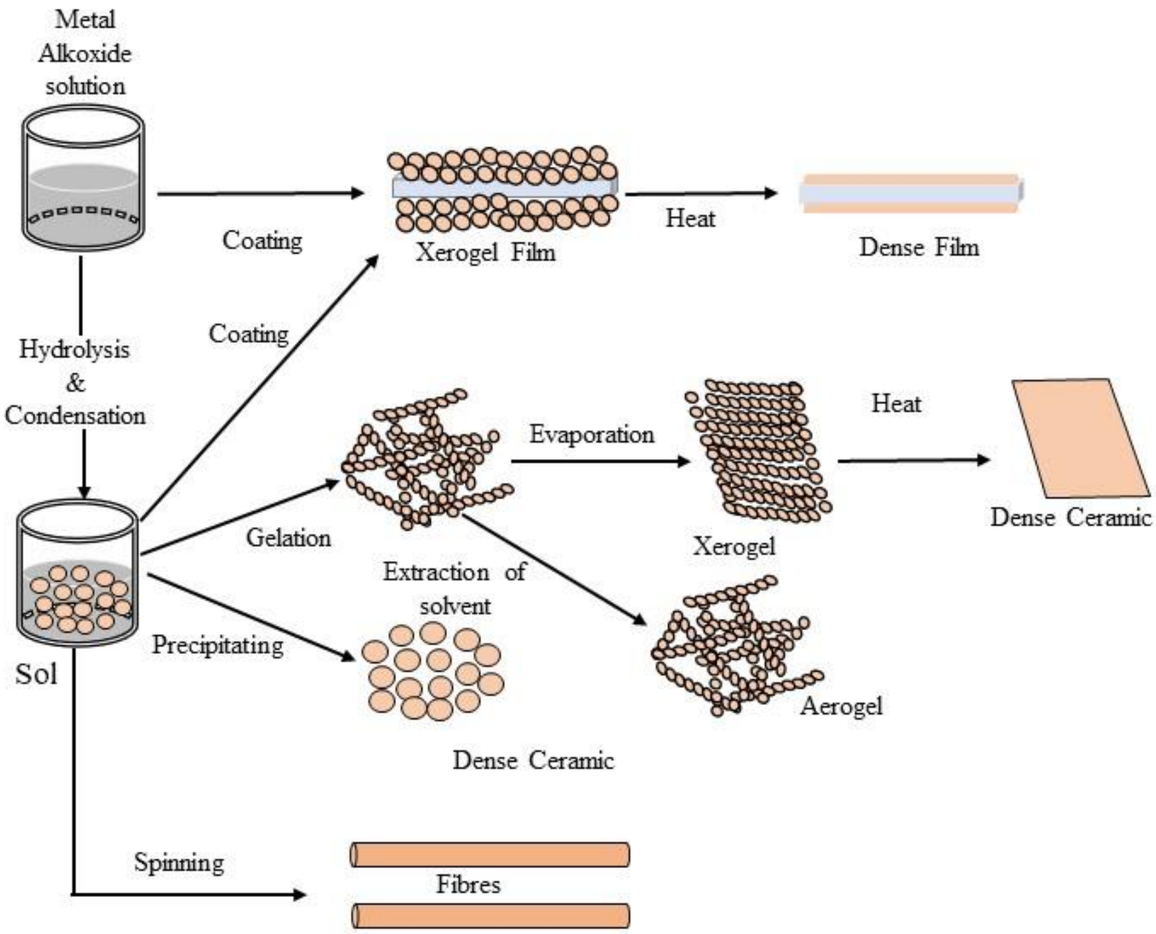

Figure 5. Sol-gel methods for nanoparticle synthesis.

3.2. Electrode material preparation

For the purpose of electrochemical sensors, there are three main options for making MIP sensing layers and composites (Figure 6): *(i)* polymerization conducted directly on the transducer surface, *(ii)* preparation of MIP or imprinted nanocomposite as powder that is coated on the electrode surface, and *(iii)* preparation of carbon paste electrode (CPE) from the mixture of carbon and MIP powder. Preparation of CPEs or deposition of imprinted nanocomposites on glassy carbon electrode (GCE) became routinely applied though we witnessed ever growing fabrication of MIP-based CPEs. "Imprinters" are more and more interested in CPEs due to their flexibility, low cost and good electrical conductivity [44].

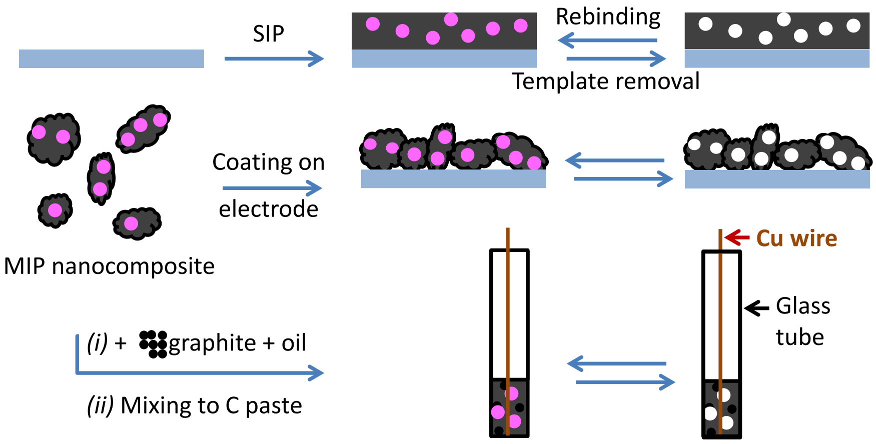

Figure 6. Three main methods to prepare MIP-based electrodes for electrochemical sensors, by direct surface initiated polymerization (SIP) on the electrode chemical (top), by preparation of MIP nanocomposite and coating it on the electrode surface (middle), and by preparing carbon paste electrode (CPE) using a mixture of MIP and carbon powders in mineral oil. MIP designates pure imprinted polymer or its corresponding composite containing nanostructures (clay, carbon, nanometal…). For the sake of simplicity, MIP means either molecularly, ion or pathogen-imprinted polymer.

Whilst preformed or in situ synthesized polymers can be deposited on the bare transducer, particularly surface-initiated polymerization requires the use of a coupling agent in order to covalently link the MIP to the transducer. In this regard, silane coupling agents, thiols and aryl diazonium salts were successfully employed. Indeed, they bear reactive functional group to bind preformed MIPs, or even a polymerization initiator group to trigger polymerization. Silanes are mostly applied to metallic surfaces with a thin oxide film or to nanoparticles, whereas thiols are mostly applied to gold electrodes. In the recent years, diazonium salts appeared as the most versatile coupling agents due to their ability to bind many more surfaces such metals, oxides, sp^2 and sp^3 carbon allotropes, insulating polymers, transparent semi-conductor electrodes to name but these materials. Furthermore, diazonium salts could be easily produced from aniline derivative precursors, bearing numerous functional groups for the attachment of polymers. For these reasons, the surface and interface chemistry of diazonium salts is reported in several patents and research publications ([45, 46]).

There are 4 polymerization methods that are compatible with the design of MIP-based sensors: thermal or controlled radical polymerization (CRP), radical photopolymerization, (electro)polymerization of conjugated monomers and sol gel polymerization.

Atom Transfer Radical Polymerization (ATRP) is the most applied type of CRP [45][‡], an easy to use method, with less specific restrictions nowadays (could be conducted in air [47]) and tolerant to most important vinylic monomers employed in MIP technology. In order to polymerize directly on the transducer, the initiator of polymerization needs to be grafted onto the metal surface [48].

Electropolymerization uses conjugated monomers as elemental bricks to assemble the polymer. The initiation of the polymerization is an oxidation of a monomer, which leads to the formation of a radical cation. Then two oxidized monomers form a dimer; the polymerization goes on with the addition of other monomers. The final polymer coating is conductive. This method is a suitable approach for the assembly of thin and insoluble films; the nanostructure can also be controlled. This is particularly important for coating electrodes.

Sol-gel polymerization consists in creating a solution of monomers and silica, the gelling of the solution on a surface will form the polymer film. This method is extremely powerful in creating films and coating [49].

Photopolymerization requires UV or visible light in order to trigger radical polymerization. Type I photoinitiators of the Irgacure type are not very suitable because most of the polymer is synthesized in bulk even though the initiator is attached to the surface [50]. Instead, Type II initiating system consists of an attached radical photoinitiator (*e.g.* N,N-dimethylaminophenyl group or a derivative) to the surface and a co-initiator that acts as hydrogen abstractor, for example benzoquinone (active under UV light) [51] or camphorquinone (active under visible, blue light) [28].

MIPs are compatible with objects of molecular (*e.g.* bacterial signaling molecule) or macromolecular size (*e.g.* proteins), however pathogens are much larger, the removal of the template after polymerization is almost impossible with big object. To adapt MIP methods to pathogen imprinting the so-called surface imprinting technique is recommended. In this strategy, only one part of the surface of pathogen is imprinted onto the polymer free surface [52]. The strategy is illustrated in Figure 7.

[‡] The combination of “molecularly imprinted polymers” and “atom transfer radical polymerization”, “reversible addition-fragmentation chain transfer”, “initiator-transfer-terminator (iniferter)” and “Nitroxide-mediated radical” polymerization returned 121, 103, 69 and 3 publications, respectively. Web of Science, last accessed 30 July 2020.

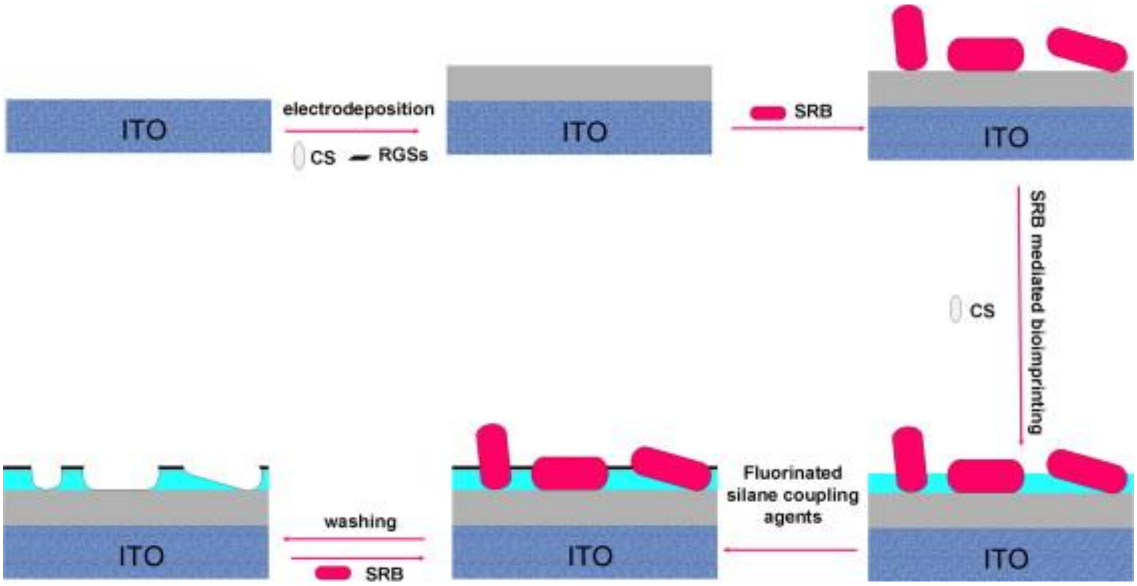

Figure 7: methods of bacteria imprinting: surface imprinting of bacteria. Adapted from [53].

4. Detection methods

Electroanalytical techniques are considered as the latest and novice friendly transduction methods, characterized by instrumental simplicity, moderate cost and portability, hence continuous rise of their utilization. Modern electrochemical methods are now sensitive, selective, rapid and easy techniques applicable to analysis in the pharmaceutical, industrial, biological and the environment fields. Electrochemical sensors can be developed for any electroactive molecules but also for the nonelectroactive molecules. Electrochemical strategies commonly used for MIP-mediated recognition of non-electroactive species are generally based on the attenuation of the electrochemical signal of a probe in solution, whose diffusion to the electrode surface is limited by the target molecules occupying the imprinted cavities of MIP coating the electrode surface [54].

Electrochemical sensors provide accurate and reliable information of the chemical composition of the materials involved. They also give reversible, uninterrupted response without agitating the sample. There is interrelationship between current/potential and the chemical composition of the components. Interaction of target analyte with the recognition matrix leads to the variation in the electrical signal. Below we consider the main electrochemical methods used in the detection of pollutants in water sources.

4.1. Cyclic voltammetry

During cyclic voltammetry (CV), the total recorded current is a sum of the capacitive and faradaic currents [55]. Both currents tend to increase with increasing sweeping speed. This relationship limits the technique sensitivity because the high capacitive current can interfere in the sensitivity of the faradaic current, which, in the linearity region, is proportional to the analyte concentration. The potential obeys the Nernst equation (Eq.1) and is therefore characteristic of a given redox process or an analyte.

$$E = E° + \frac{RT}{nF} \ln \frac{[RED]}{[OX]} \qquad (1)$$

where E, cell potential; E°, standard potential of a half-reaction; R, universal gas constant; T, temperature; n, number of electrons (eq. mol^{-1}) involved in the half-reaction; F, Faraday constant; [RED] = activity of the reduced species; and [OX] = activity of the oxidized species.
Thus, CV can be used for quantitative determinations. However, because of its limitations, it is more generally used for exploratory purposes, that is, to determine the redox process of different analytes. To minimize the contribution of the capacitive current and therefore increase the sensitivity of voltammetric methods, potential impulse (or pulse) methods were developed, including differential pulse voltammetry and square wave voltammetry (SWV). CV helps us to understand the basic redox characteristics of the analyte or recognition matrix. It can be used to monitor the variations in the composition of recognition matrix. Using this method, a variety of sensors and biosensors may be applied, studied and modified so as to determine the substance to be analyzed. Molecular printing is the novelty of these devices, as they have numerous improved features: high sensitivity, short response time, simplicity of electronic interface, portable tools.

4.2. Differential Pulse Voltammetry

Differential pulse voltammetry (DPV) is a technique that involves applying amplitude potential pulses on a linear ramp potential. In DPV, a base potential value is chosen at which there is no faradaic reaction and is applied to the electrode. The base potential is increased between pulses with equal increments. The current is immediately measured before the pulse application and at the end of the pulse, and the difference between them is recorded (Figure 8a). DPV is a differential technique similar to the first derivative of a linear voltammogram in which the formation of a peak is observed for a given redox process In DPV, the peak potential, Ep, can be approximately identified with the half-wave potential (E1/2), which corresponds to the potential at half the wave height. Increasing the irreversibility, Ep deviates from E1/2 as the base of the peak widens and its height decreases. The DPV is therefore a graph of differences between measured currents and applied potentials (Figure 8b). . In general, pulse techniques, such as DPV, are more sensitive than the linear sweep methods because there is minimization of the capacitive current. The best responses obtained with the use of DPV, compared to normal pulse voltammetry, are on solid electrodes, especially those involving organic compounds. Since they are usually adsorbed by the electrode, it is possible that a differential technique discriminates the effects that are more or less constant before and after the application of pulses.

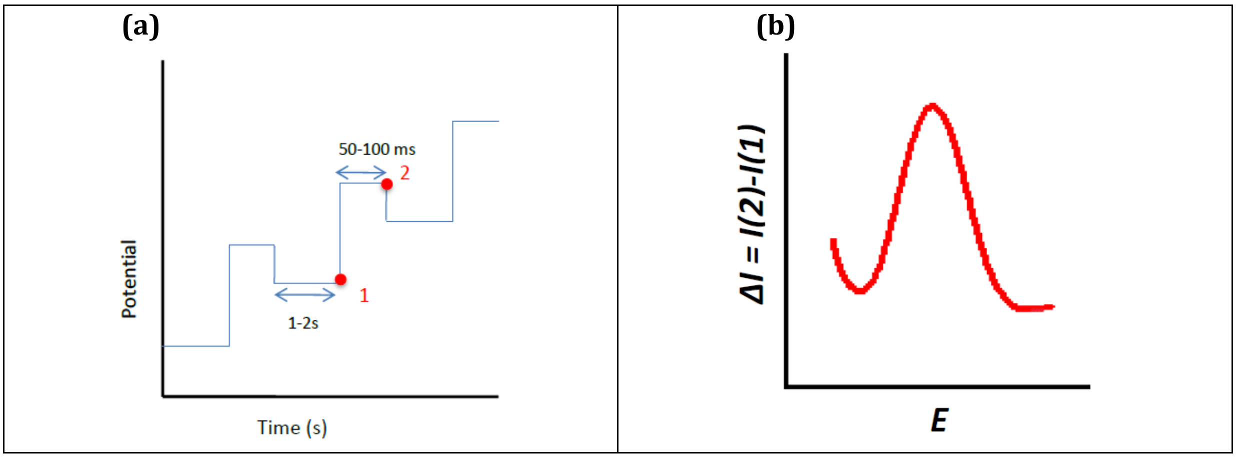

Figure 8. (a) Typical response of a differential pulse voltammogram. (b) Diagram of the application of pulses in the DPV technique.

4.3. Square wave voltammetry

In addition to DPV, square-wave voltammetry (SWV) is a very sensitive electrochemical technique. The detection limits can be compared with those of chromatographic and spectroscopic techniques [55].

The analysis of the characteristic parameters of this technique also enables the evaluation of the kinetics and mechanism of the electrode process under study. It is based on the principle that the signal-to-noise ratio increases by the square root of the scan rate. This improvement in the signal is a function of the time between pulse application and the current measurement. More specifically, the timing for the SWV is frequency dependent, so when the frequency increases, the time constant decreases and the measured faradic current is increased, giving more sharp and defined peaks to the voltammogram [56]. Faster analysis speed results in less consumption of electroactive species and less electrode surface blockage problems.

Figure 9a shows the application of pulses in the SWV technique, whereas details of the potential application of SWV are shown in Figure 9b-c, with the definition of the used parameters and the theoretical voltammograms associated with a reversible system (Figure 9b) and an irreversible system (Figure 9c).

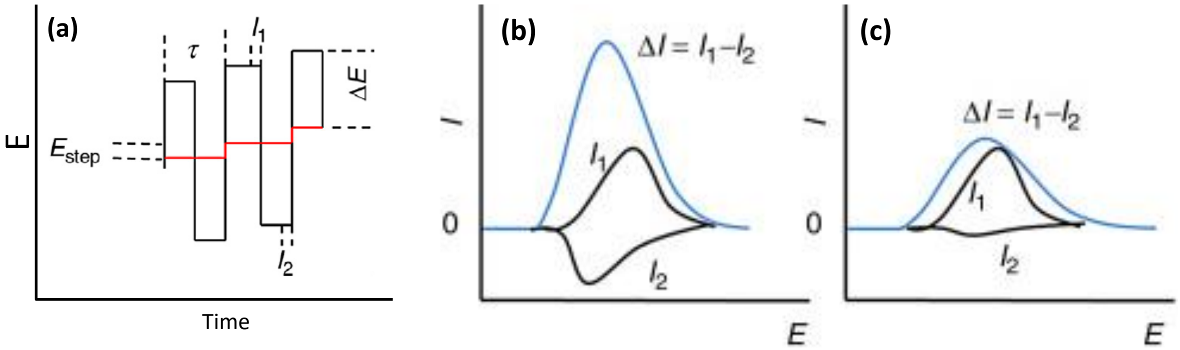

Figure 9. (a) Diagram of the application of pulses in the SWV technique. Schematic square wave voltammogram, where (b) represents a redox process of a reversible system and (c) represents that of an irreversible system. Adapted from [57]

Current–potential curves display well-defined profiles and are usually symmetrical. Peaks corresponding to the oxidation or reduction of the electroactive species at the electrode surface can be obtained in the same experiment; and by subtraction their difference. Hence for a reversible system, the current obtained is much higher. The SWV technique has been used in the development of numerous sensors and biosensors because of its high sensitivity and selectivity. It is currently of great interest to the detection of environmental pollutants, such as heavy metals, and other chemical contaminants that are part of the environmental liability in contemporary societies.

4.4. Amperometric sensors

In amperometric sensors, a constant electric potential is applied to the electrochemical cell and a corresponding current appears because of the redox reactions that occur on the surface of the working electrode. This current can be used to quantify the reactions involved. Amperometric sensors have the advantages that they provide a signal, which varies linearly with the concentration of the analyte, fast response time, high reproducibility, and high sensitivity. In addition, amperometric sensors are compact and can be used for the continuous monitoring. For these reasons, existing portable sensors were majorly constructed using amperometry technique.

4.5. Stripping voltammetry

Stripping (or pre-concentration) techniques have been used for cations and some anions and complexing neutral species, the detection limit being of the order of 10^{-10} M. They are thus excellent techniques for the determination of chemical species at trace levels, and also for speciation studies. At these levels the purity of the water and of the reagents used in the preparation of the supporting electrolyte are extremely important.

The process effectively consists of two or sometimes three steps:

- Deposition or adsorption of the species on the electrode during a time t (preconcentration step). This step occurs under potential control or at open circuit;
- Change to an inert electrolyte medium. This step can sometimes be unnecessary;
- Reduction/oxidation of the species that was accumulated at the electrode. This can be achieved by varying the applied potential, registering a current peak (or its integral) proportional to concentration.

Important applications for trace metals are the use of anodic stripping voltammetry (ASV) to determine trace quantities of copper, cadmium, lead and zinc, and adsorptive stripping voltammetry (AdSV) of trace quantities of nickel and cobalt—pre-concentration by adsorption accumulation of the oxime complexes followed by reduction to the metal is employed, as reoxidation of these metals in ASV is kinetically slow and does not lead to well-defined stripping peaks.

The use of pulse techniques can substantially lower the limits of detection of ASV (to 10^{-12} M) and increases the sensitivity. The two most commonly used pulse techniques are differential pulse and square wave anodic stripping voltammetry (DPASV and SWASV, respectively). A previous work describes in more detail these different techniques for the analysis of heavy metals [58].

4.6. Electrochemical impedance spectroscopy

Electrochemical impedance spectroscopy (EIS) is a technique used to analyse electrochemical processes occurring in the interface between the electrode and the electrolyte solution. It is based on the application of a small sinusoidal voltage to the working electrode and measuring the complex impedance at the electrode/electrolyte interface over an appropriate frequency range: Z(ω) (ω= 2πf is) [59]. There is two different ways to represent the impedance spectrum (Figure 10) : The "Nyquist plot" (left side) that represents the real and imaginary parts of Z(ω) using cartesian coordinates and the "Bode plot" (right side) where phase is plotted as a function of log of the frequency. This representation has great advantages for observing phase margins in which the system becomes unstable (violent phase or magnitude changes). The Nyquist plot provides insight into the possible mechanism or governing phenomena in an equivalent circuit model system [60].

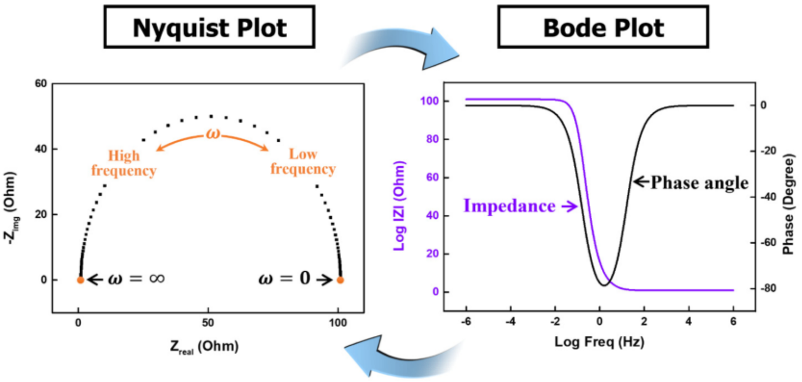

Figure 10. Electrochemical Impedance Spectroscopy representation by Nyquist plot (left) and Bode plot (right). Reproduced from [60].

EIS-based sensors have been reported for countless applications such as the detection of cancer and other disease biomarkers, bacteria, polluting agents, water contamination and toxins [61, 62]. Several biosensors have been constructed by applying the core concepts of EIS in combination with biological recognition elements. The use of affinity-based biosensors in EIS makes it convenient for the direct and label-free electrochemical immunosensing and potentially speeding up the analysis.

4.7. Comparison of electrochemical techniques

Table 3 compares various electrochemical techniques. As it will be shown below in case, DPV and SWV are most applied techniques for tracking redox species (ions and molecules), whereas bacteria will best be tracked with impedance measurements.

Table 3. Principles, features and applications of electrochemical techniques exploited in MIP-based electrochemical sensors.

Electrochemical technique	Principal	General features and applications
Cyclic voltammetry	Measured current is as a function of the linear applied potential	CV provides essential redox processes and informations concerning the analysis (matrix, analyte, and electrode). Not very useful for quantitative determinations.
Differential Pulse Voltammetry	The current is measured between increased pulses of potential with equal increments.	Low capacitive current leads the enhancement of the sensitivity. Very low and competitive LOD values. Usually applied in the case of irreversible systems or in systems presenting slow-reaction kinetics
Square Wave Voltammetry	Current is determined when an increasing square wave potential is applied	Low capacitive current leads the enhancement of the sensitivity. Very low and competitive LOD values. Often applied for the study of reversible or rapid reaction kinetics systems
Amperometric techniques / Chronoamperometry	constant electric potential is applied to and a corresponding current appears	Very useful for the continuous monitoring. device is suited to miniaturization and portability. Difficulty to sense the existence of multiple target analytes in the media.
Stripping voltammetry	A step of analyte pre-concentration precede its stripping by scan potential application	Very powerful technique for trace metals and some complexing neutral species determination. Require many optimisations and experimental condition preparations for each application in order to be effective.
Electrochemical impedance spectroscopy	small sinusoidal voltage is applied and complex impedance is measured at the electrode/electrolyte interface	High sensitivity and specificity. Numerous applications (pathogens, biomolecules, water contamination and toxins detection). Non-specific adsorption onto the electrode surface. Often requiring a Faraday cage to reduce noise. the need for theoretical simulation for data analysis

5. Applications of imprinted polymer-based electrochemical sensors

5.1. Tracking pesticides with molecularly imprinted polymers

5.1.1. Pesticide imprinted sol-gels (PISGs)

Various sol-gel based sensors were realized for pesticide detection and quantification. Beduk *et al.* have designed an inkjet-printed ZnO sol-gel modified PEDOT:PSS/Nafion disposable sensor for the selective detection of hydrazine [63]. Chronoamperometry and cyclic voltammetry techniques were investigated for the determination of low concentrations of hydrazine and for selectivity tests. Results indicate that the oxidation of hydrazine is catalyzed by ZnO particles, and that the modification of a PEDOT:PSS surface with ZnO sol-gel improves the sensor's sensitivity and stability. The limit of detection (LOD) and sensitivity values of the designed sensor were of the order of 5 µM and 0.14 $\mu A.\mu M^{-1}.cm^{-2}$, respectively.

Organophosphorus (OPs) compounds were extensively used as insecticides, fungicides and herbicides. Exposure to OPs inhibits the activity of Acetylcholinesterase (AChE), an enzyme which plays a key role in the appropriate functioning of the central nervous system [64]. OPs pesticides act generally as anti AChE causing over-accumulation of acetylcholine and thus cholinergic toxicity [65]. Several Electrochemical biosensors, based on inhibition of (AChE), were thus designed for OPs detection [66].

Hu *et al*. designed an AChE sensor based on titanium dioxide (TiO_2) sol-gel carrier for dichlorvos (DDVP) detection by CV and DPV [67]. In this study, a solution of TiO_2 and chitosan (CS) was drop-coated on the surface of a glassy carbon electrode. After drying in air and further formation of a thin film on the surface of the electrode, a solution containing AChE and CS (0.5 %) is dropped on the functionalized CGE. The designed biosensor exhibits a linear response in the concentration interval 1.13 nM to 22.6 µM, and a limit of detection of order of 0.23 nM.

Cui *et al*. [68] designed an electrochemical AChE biosensor for the detection of an OP model, dichlorvos (DDVP) in cabbage juice samples. In this study, an rGO/GC electrode was coated with TiO_2-CS solution and then left in air for gelation. This step was followed by the electrodeposition of a chitosan layer prior to the immobilization of AChE (in a PBS solution containing 1% bovine serum albumin). DPV results indicate that the linear range was from 0.036 µM (7.9 ppb) to 22.6 µM and that its LOD was equal to 29 nM (6.4 ppb).

DDVP detection was also investigated by Zhang *et al*. [69] who have designed an electrochemical biosensor based on silver nanowires (AgNWs)/ glassy carbon, TiO_2 sol-gel–CS, graphene and AChE. The electrochemical activity of this biosensor was found dependent on the oxidation of thiocholine (TCl), an enzymatic product obtained from AChE hydrolysis. Subsequently, TCl oxidation was investigated by DPV. This biosensor was found to be stable and selective in the presence of several interfering species; LOD was of order of 7.4 nM (1.64 ppb).

Song *et al.* [70] employed a strategy based on citrate-capped gold nanoparticles (AuNPs)/(3-mercaptopropyl)-trimethoxysilane (MPS)/Au electrode for the selective detection of carbamate. The authors reported a 3D-MPS sol–gel network which was assembled on Au electrode surface via Au-S bond. The CV response of the biosensor was found dependent on the activity inhibition of AChE in the presence of the carbaryl (1-naphthyl methylcarbamate). This sensor revealed a linear range from 0.003 to 2 mM, a limit of detection of 1 nM and a sensitivity of 32.0 $\mu A.cm^{-2}.mM^{-1}$. The proposed biosensor shows good reproducibility and long-term storage stability.

Maulidiyah *et al* [71] modified a carbon paste electrode (CPE) with a TiO_2 sol-gel for fipronil detection in real samples. To prepare the working electrode, the authors mix TiO_2 nanoparticles (obtained from the crush of anatase crystal) with carbon and paraffin oil, prior to heating at 80°C. The composite was after that entered in probe glass connected by Cu wire as a conductor and also tip electrode. Cyclic voltammetry results indicate that the TiO_2-CPE sensor presents a limit of detection of 34.0×10^{-5} µM and 23 days of lifetime.

Jayaraj *et al.,* [72] prepared, via a simple sol–gel technique, a 3D flower-like gadolinium molybdate (Gd_2MoO_6; GdM) and used it as a bifunctional catalyst for photocatalytic degradation and electrochemical detection of fenitrothion (FNT). The synthesis procedure and the further applications are presented in Figure 11.

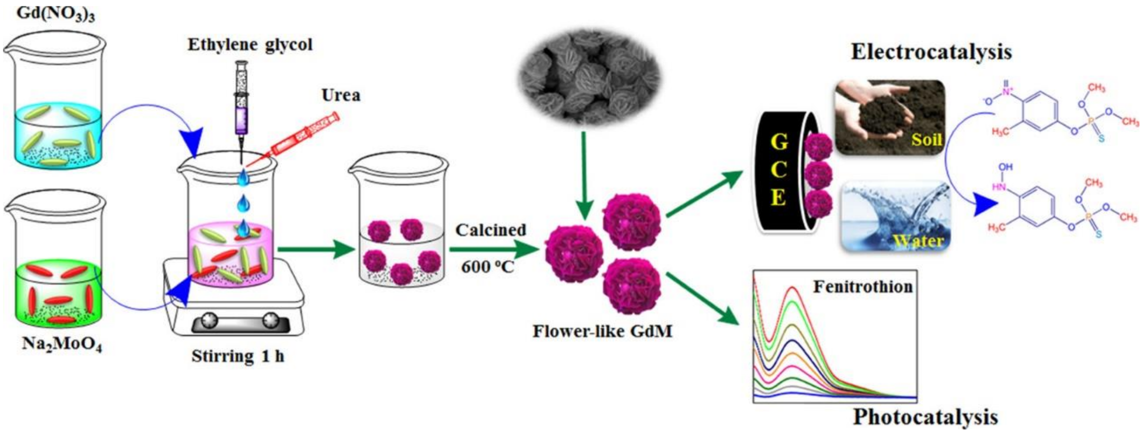

Figure 11. Overall synthesis procedure of flower-likeGDM and its electrocatalytic and photocatalytic applications. Reproduced with permission from [72].

DPV measurements indicate that GdM catalyst plays a significant role in the electrochemical reduction of FNT. The flower-like GdM-modified GCE exhibits a wide linear range (0.02–123; 173 – 1823 µM), a sensitivity of order of 1.36 $\mu A.\mu M^{-1} cm^{-2}$ and a limit of detection of 5 nM. Additionally, the GdM photocatalyst could degrade above 99% of FNT under UV light irradiation with good stability even after five cycles.

Xue *et al.* [73] modified glassy carbon electrodes (GCEs) with multi-walled carbon nanotubes (MWCNTs)@TiO_2 and Carboxymethyl chitosan (CMCS) to detect trichlorfon pesticide in fruits. The optimum mass ratio composition was found equal to 10/10/80 for MWCNTs/TiO_2/CMCS. The analytic performances of the designed sensor were investigated by cyclic voltammetry and differential pulse voltammetry. Electrochemical results indicated a wide linear range, from 10^{-5} to 10^{-11} $mol.l^{-1}$, a sensitivity of 0.5077 $\mu A.M^{-1}$, a limit of detection of order of 4×10^{-7} $mol.l^{-1}$ and a recovery of 98 %.

5.1.2. Pesticide imprinted vinylic polymers (PIVPs)

The literature reported the design of MIP based electrochemical sensors for selective detection of cypermethrin (CPM), a synthetic pyrethroid pesticide widely used in agriculture and spot treatment for insects' control. CPM may however induce neurotoxicity by modulating the level of gamma-amino butyric acid [74]. Leepheng *et al.* [75] designed a molecularly imprinted electrochemical sensor for CPM detection in vegetable juice. In this work, the authors used methyl methacrylate (MMA), ethylene glycol dimethacrylate (EDGMA), 2,2′ azobis(2-methylpropronitrile) (AIBN), as the functional monomer, the cross-linker and the initiator, respectively. The polymerization was carried-out at 70°C for 2 h. This step was followed by dropping CPM-MIP onto screen-printed electrodes (SPE) at a controlled temperature of 60°C during 90 min. The templates were removed by ethanol and deionized water. Cyclic voltammetry measurements indicate that CPM-MIP/SPE sensor presents a limit of detection of 15 ppb and a sensitivity of 0.094 $\mu A.ppm^{-1}$.

Cypermethrin (CYP in this study) detection was also reported by Li *et al,* [76] who prepared a solution of Ag-N@ZnO/CHAC from coconut husk (CHAC), dropped it on the surface of a glassy carbon electrode and dried it under infrared lamp, prior to the MIP electro-polymerization. Two functional monomers were investigated in this study: resorcinol and dopamine. CYP extraction was performed by the immersion of the coated electrode in 0.1 M NaOH and by scanning between −1.0 V and +1.0 V for 10 cycles. CV measurements were performed to investigate the effects of double monomers use, to optimize the ratio between template and monomers, to determine the analytical performances of the sensor and for selectivity tests. The designed MIP based sensor was selective of CYP and presents a LOD of order of 6.7×10^{-14} M.

Glyphosate (Gly), a synthetic herbicide, is probably the most widely used pesticide worldwide. In 2015, the World Health Organization’s International Agency for Research on Cancer classified glyphosate as potentially carcinogenic to humans. This health concern has motivated the realization of numerous chemical sensors to track glyphosate in water samples, soil, air and body fluids. In the field of MIP-based electrochemical sensors, Zouaoui *et al.* [77] designed a sensitive and selective sensor, in which a chitosan (CS)-Gly-MIP was electrodeposited, by cyclic voltammetry (from -1.5 to 0.5 V at a scan rate of 80 mV/s) onto a gold microelectrode surface. Cross-linking of the polymeric matrix was performed by incubating the (GLY +CS)/Au in a solution of H_2SO_4 for 1 hour. Gly templates extraction was done by incubating the microelectrodes in a protic solution acetic acid/methanol (1:1, v/v) for 30 min. The sensing properties of the designed sensor were followed-up by electrochemical impedance spectroscopy and cyclic voltammetry. Results indicate a limit of detection of 0.001 pg/ml and a linear range from 0.31 pg/ml to 50 ng/ml.

Glyphosate detection was also investigated by Mazouz *et al*. [78] who have designed an electrochemical sensor functionalized with polypyrrole (PPy)-MIP electrodeposited by chronoamperometry (CA) on the surface of a gold electrodes. In order to reduce the oxidation potential of pyrrole during MIP elaboration, a thin polypyrrole blocking layer was deposited on Au surfaces. Here also Gly templates extraction was done by incubating the electrodes in a protic solution acetic acid/methanol (1:1, v/v) for 30 min. SWV was investigated to optimize the MIP synthesis and to determine the metrological performances of the designed sensor. The sensitivity was equal to (75 ± 41) µM/nM and the LOD was of order of 1 pM. The dissociation constants, related to the affinity between polypyrrole and glyphosate, were calculated from the fit of the calibration curve with a combined one site/ Hill model. They were found of order of Kd_1 = (0.7 ± 0.3) pM and Kd_2 = (1.6 ± 1.4) µM, which indicate a high affinity between Gly analytes and the cavities created in the PPy polymeric matrix.

MIP-based electrochemical sensors were also designed for the detection of organophosphorus compounds. Aghoutane *et al.* [79] designed an acrylamide-MIP on screen-printed gold electrodes to quantify malathion (MAL) in olive fruits and oils. In this study, a solution of MAL templates and bisacrylamide monomers was incubated at 4°C during 6 h in the presence of N, N, N, N-tetramethyl ethylenediamine and ammonium persulfate as catalysts. Polymerization was carried out overnight in an oven at 74°C. The extraction step was done with a solution of methanol and acetic acid solution (9/1 : v/v) for 10 min. Cyclic voltammetry, differential pulse voltammetry and electrochemical impedance spectroscopy techniques were used to investigate the analytical performances of the designed sensor. The MIP based device exhibited satisfactory selectivity, a dynamic concentration range of (0.1 pg mL^{-1}-1000 pg.mL^{-1}), a limit of detection of 0.06 pg.mL^{-1} and a recovery rate of 87.9%.

Hassan *et al.* [80] reported methyl parathion electrochemical detection in fish by pre-concentrating the pesticide on magnetic MIP and further readout on magneto-actuated electrode by square wave voltammetry. Magnetic-MIP was prepared using Fe_2O_3 as magnetite nanoparticles core, methacrylic acid as a functional monomer, EGDMA as crosslinking monomer, 2,2-azobis-isobutyronitrile (AIBN) as a radical initiator, and methyl parathion as a template. Methyl parathion extraction was done using a Soxhlet and methanol / acetic acid (9 / 1). SWV results indicate that magnetic-MIP/m-GEC sensor presents a LOD of 1.22×10^{-6} mg L^{-1} and recovery values ranging from 89.4% to 94.7%.

Wang *et al.* [81] fabricated a molecularly imprinted electrochemical sensor for methyl parathion (MP) quantification in vegetables and fruits matrixes. The sensor was designed using glassy carbon (GCE) and AuNPs to improve the electrical conductivity and enhance the electron transfer. The imprinted sensor was prepared in acetate buffer solution containing quercetin, resorcinol, $KclO_4$, and methyl parathion templates. The composite was after that electroplated, onto Au/GCE electrode surface, by cycling in the potential range from -0.2 to 0.9 V at a scan rate of 0.05 V/s. MP templates extraction was done by submerging the electrode in ethanol acid solution for 5 s. CV Electrochemical results indicated a limit of detection of 0.01 µM, a good selectivity and a recovery range from 87.7 to 124.8 %.

Methyl Parathion detection was also investigated by He *et al.* [82] who have synthesized the MIP by free radical polymerization in chloroform. Zinc porphyrin, ethylene glycol dimethacrylate (EGDMA) and AIBN were used as functional monomer, cross-linker and initiator, respectively. Under the optimized experimental conditions, DPV results indicate that the sensor presents a limit of detection of 31.6 nM and that it is stable over 30 days.

Xu *et al*. [83] realized a disposable electrochemical sensor for sensitive and selective detection of phosalone insecticide in agricultural products and environmental samples. A home-made carbon paste microelectrode (CPME) was modified with Zr−based metal−organic framework catalyst (Pt−UiO−66) and a mesoporous MIP. The latter was synthesized onto Pt-UiO-66/CPME by electropolymerization and a subsequent sol−gel process. SWV results revealed that a mixture of acetonitrile/methanol (1:1, v/v) can efficiently extract the templates from the polymeric matrix and that the designed sensor exhibits a linear range in the domain 0.50 nM–20 mM and a limit of detection (LOD) of 0.078 nM.

Amatatongchai *et al*. [84] designed a selective profenofos sensor in which a GCE was modified with SiO_2-vinylcarboxylated carbon nanotubes (CNTs) and then with molecularly imprinted polymer shells. The synthesis procedure is presented in Figure 12.

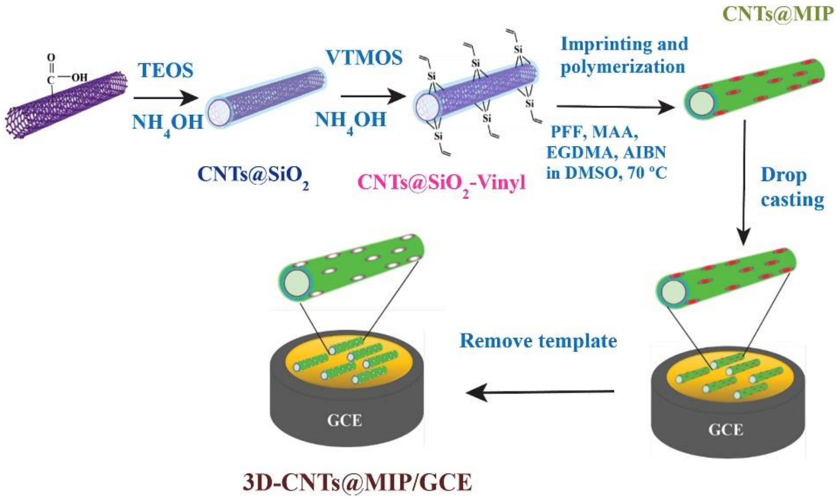

Figure 12. Schematic representation of the 3D-CNTs@-MIP preparation and further fabrication of the MIP sensor. Used with permission from [84].

The 3D-CNTs@MIP sensor exhibited a wide linearity range (01–200 µM), a low limit of detection, 2 nM, and a linear sensitivity, calculated from the slope of the amperometric response of 0.573 $A.M^{-1}$.

Zhang *et al.* [85] study concerns the detection of imidacloprid residue with a MIP for which the functional monomer was p-vinylbenzoic acid (VBA) and the crosslinker was ethylene glycol dimethacrylate (EGDMA). The designed sensor was fabricated using graphene and modified glassy carbon electrode to improve the stability and the imprinting of the film. Linear sweep voltammetry (LSV) measurements indicate that the designed electrochemical sensor was sensitive and selective and that it achieved a detection limit of 0.10 µM, a limit of quantification of 0.33 µM and a linear range from 0.5 to 15 µM.

In 2016, Kumar *et al* [86] used superparamagnetic iron oxide nanoparticles coated with vinyl silane (silane@SPIONs) and molecularly imprinted star polymers (MISP) to detect and remove Mancozeb (MCZ) from soil and vegetable samples. The authors have used itaconic acid as functional monomer and ethylene glycol dimethacrylate (EGDMA) as crosslinker. Imprinted star polymer synthesis steps are presented in Figure 13.

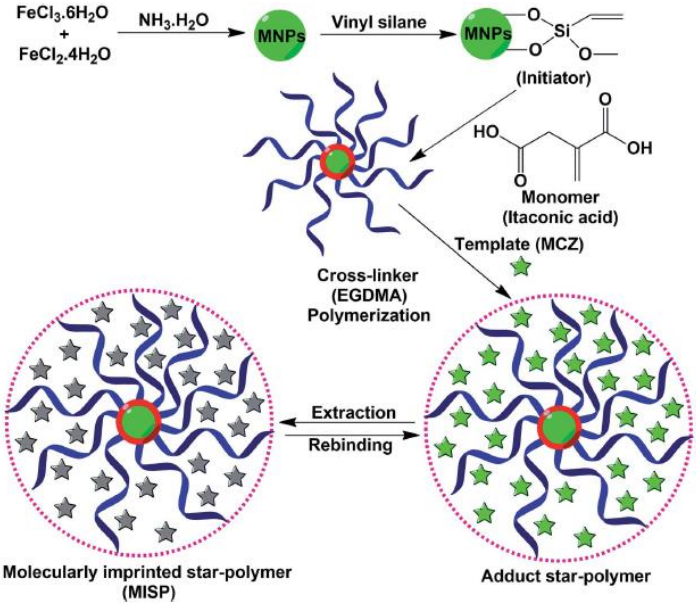

Figure 13. Different steps of fabrication of mancozeb-imprinted star polymer. Used with permission from [86].

Quantitative measurements, investigated with square wave stripping voltammetry indicate that the electrochemical sensor has a wide linear range from 5.96 to 257.0 $mg.L^{-1}$ and a detection limit of 0.96 $mg.L^{-1}$. The sensor exhibited excellent selectivity in the presence of different interferents and good stability/reusability after 6 months storage.

El-Moghazy *et al.* [87] developed a sensitive AChE biosensor for pirimiphos-methyl detection in olive oil samples after a simple liquid-liquid extraction. In this study, screen printed electrodes (SPE) were functionalized with electrospun chitosan - polyvinyl alcohol (CS-PVA) blend nanofibrous membranes (NFM), which were activated with glutaraldehyde1%, prior to incubation with AChE. Inhibition assays were then carried out using pirimiphos-methyl oxon. Amperometric results indicate that designed (AChE/ CS-PVA NFM/SPE) sensor was stable and reproducible during 10 consecutive measurements. The LOD was of order of 0.2 Nm, corresponding 6.10^{-5} ppm.

5.1.3. Pesticide imprinted conductive polymers (PICPs)

Dong *et al.* [88] reported an electrochemical AChE biosensor based on microporous organic polymers (MOP) for methyl parathion and paraoxon detection in lettuce samples. Herein, phloroglucinol-based MOP was prepared via simple microwave synthesis and then drop coated onto the surface of a carbon paste electrode. AChE was then added and subsequently immobilized by Nafion. The synthesis process and detection procedure are displayed in Figure 14.

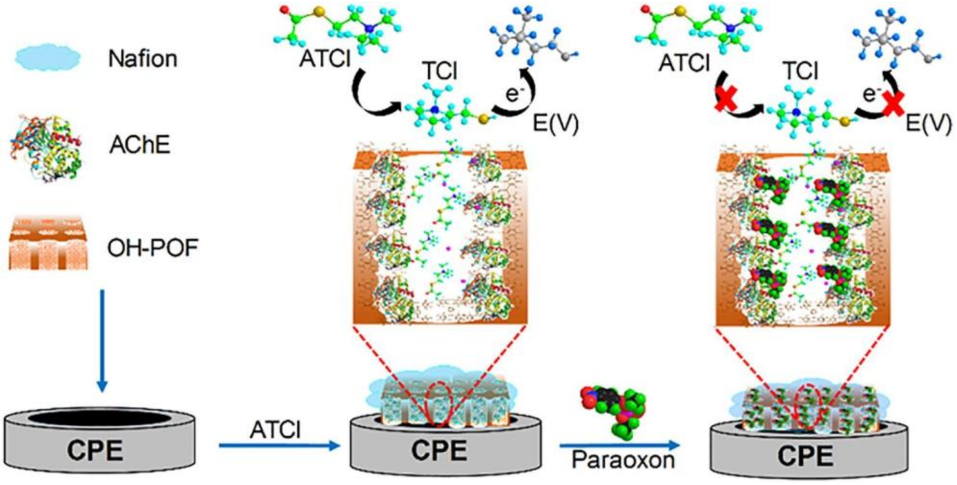

Figure 14. Illustration of the fabrication process of the NF/AChE/OH-POF/CPE biosensor. Used with permission from [88].

DPV electrochemical results were related to the oxidation of thiocholine, produced from ATCI hydrolysis in the presence of AChE. The limits of detection for methyl parathion and paraoxon, were of order of 1.5 × 10^{-13} g.mL^{-1} and 3.4 × 10^{-14} g.mL^{-1} respectively. The linear ranges varied between 5.0 × 10^{-13} to 1.0 × 10^{-8} g.mL^{-1} for methyl parathion and from 1.0 × 10^{-13} to 1.0 × 10^{-9} g.mL^{-1} for paraoxon.

Yassa *et al*. [89] modified a graphite electrode with thienopyrrole based conjugated poly[1-(5-(4,8-bis(5-(2-ethylhexyl)thiophen-2-yl)benzo[1,2-b:4,5-b']dithiophen-2-yl)furan-2-yl)-5-(2-ethylhexyl)-3-(furan-2-yl)-4H thieno[3,4-c]pyrrole-4,6(5H)-dione] (PFTBDT) and carbon dots (CDs) for the detection of catechol phenolic compounds used in pesticide synthesis. In this study, PFTBDT was synthesized via stille polycondensation reaction and then coated on CDs modified electrode. This step was followed by the immobilization of laccase enzyme onto the modified electrode, using glutaraldehyde 1% as a cross-linker agent. Several parameters were optimized in this study, such as the amounts of carbon dots, of PFTBDT, of enzyme and the pH of the operating media. Amperometric measurements indicate that the proposed biosensor exhibits a limit of detection of 1.23 μM, a sensitivity of 737.4 $\mu A.mM^{-1}.cm^{-2}$ and a wide range between 1.25 to 175 μM.

Akdag *et al*. [90] designed an electrochemical AChE biosensor for Paraoxon detection using polypyrrole and chitosan modified platinum (Pt) electrode. The authors electropolymerized pyrrole monomers, by cyclic voltammetry, on platinum electrode (Pt/PPy) and then coated it with a chitosan solution. The chi/Pt/PPy modified electrode was after that incubated in a buffer solution containing glutaraldehyde in order to immobilize AChE enzyme. The sensing properties of the biosensor were monitored by DPV. LOD was of order of 0.17 nM and the sensor exhibited 72 % of stability after 60 days.

Kondawar *et al*. [91] modified a graphite electrode surface with two layers of conducting polymers to design an AChE biosensor for Acephate quantification. In this study, pyrrole monomers were first electrochemically deposited by CV, in the −0.6-0.9 V range for 10 cycles at scan rate 50 mV/s, onto a graphite electrode. Subsequently, aniline with carbon nanotubes (CNTs) was electropolymerized by CV on the polypyrrole modified graphite electrode surface, prior to the immobilization of AChE. Chronoamperometry results indicated that the biosensor presents a limit of detection of 0.007 ppm.

Turan *et al*. [92] designed a butyrylcholinesterase (BChE) amperometric biosensor for the quantitative determination of paraoxon in milk and tap water. In this work, 5,6-bis(octyloxy)-4,7-di(thieno[3][3,2-b]thiophen-2-yl)benzo[c][1,2,5]oxoadiazole (TTBO) was electropolymerized, by cyclic voltammetry, on graphite electrode surface prior to the immobilization of silver nanowires (AgNWs) and then BChE. Glutaraldehyde was used to improve the electron transfer, the sensitivity and the selectivity towards paraoxon. The poly(TTBO)/AgNWs/BChE biosensor revealed a limit of detection 0.212 μM and a sensitivity of 8.076 $\mu A\ \mu M^{-1}\ cm^{-2}$.

Guler *et al*. [93] constructed a conducting polymer on a glassy carbon electrode (GCE) for the quantification of malathion in parsley leaves samples. The working electrode was prepared by electropolymerizing [2,2 ;5′ 2″]-terthiophene-3-carbaldehyde) (PTT) monomers on the GCE by cyclic voltammetry (in the range from 0.8 to 1.5 V). After that, AChE was immobilized on the PTT film surface and covalently cross-linked by glutaraldehyde. The biosensor response was dependent on the oxidation of thiocholine, which is the hydrolysis compound of acetylthiocholine iodide, catalyzed by AChE activity. CV electrochemical results indicated that the limit of detection was of order of 4.08 nM and that the sensitivity and the recovery were equal to 183.2 µA/mM and 97%, respectively.

Bhardwaj *et al*. [94] designed an immunosensing platform on the basis of a thin film assembly of Cu-MOF ($Cu_3(BTC)_2@SiO_2$) and 2-amino terephthalic acid (NH_2-BDC) doped polyaniline (PANI) to detect traces of atrazine. In this study, the conducting film was synthesized by mixing NH_2–BDC and aniline monomers in ice bath and then by spin-casting the mixture onto a four electrode sensor surfaces. This step was followed by the spin-casting of $Cu_3(BTC)_2@SiO_2$ on BDC-PANI electrode surface and by annealing at 100 °C to establish a good bonding. The modified thin film was then bioconjugated with anti-atrazine antibodies. This immunosensor was reproducible and reliable and exhibited a limit of detection of 0.01 nM.

Salih *et al*. [95] modified the surface of a carbon paste electrode (CPE) with p-Phenylenediamine (p-PD) conducting polymer and ionic liquid (IL) for carbaryl detection in spring water and fruit samples. In this work, different amounts of IL were mixed with graphite and paraffin oil to fabricate IL modified carbon paste electrode (IL/CPE). Two p-PD electropolymerization strategies on IL/CPE surfaces were investigated: *(i)* by cyclic voltammetry in the range -0,4 to 0,8 V for 40 cycles; and by *(ii)* potentiostatic mode at a fixed potential 0.7 V during 120 s. Several experimental conditions were tested and optimized: the ionic liquid ratio in paraffin oil, the number of polymerization cycles, pH and the preconcentration duration. DPV results indicated that the Poly-pPDs-IL/CPE sensor presents a limit of detection of 0.09 $mmol.L^{-1}$ and reasonable recovery values between 96 to 117.4%.

5.1.4. Summary of pesticide imprinted polymer-based electrochemical sensors

Table 4. Performances of handpicked pesticide electrochemical sensors.

Pesticide	Sensing material	Method of detection and conditions	LOD, Sensitivity (s), Detection range (DR)	Refs
Hydrazine	ZnO, NF	CV	LOD = 5 μM S = 0.14 μA.μM^{-1}.cm^{-2}	[63]
Dichlorvos	TiO_2/CS	CV, DPV	LOD = 0.23 nM DR = 1.13 nM to 22.6 μM	[67]
Dichlorvos	TiO_2/CS	DPV	LOD = 29 nM DR = 0.036 μM to 22.6 μM	[68]
Dichlorvos	TiO_2/CS	DPV	LOD = 7.4 nM	[69]
Carbamate	MPS	CV	LOD = 1 nM S = 32.0 μA.cm^{-2}.M^{-1}	[70]
Fipronil	-	CV	LOD = 34×10^{-5} μM	[71]
Fenitrothion	GdM	DPV	LOD = 5 nM S = 1.36 μA.μM^{-1} cm^{-2}	[72]
Trichlorfon	TiO2/CMCS	CV, DPV	LOD = 4×10^{-7} M S = 0.5077 μA.M^{-1}	[73]
Cypermethrin	MMA (FM), EDGMA (CL), AIBN (In)	CV	LOD = 15 ppb S = 0.094 μA.ppm^{-1}	[75]
Cypermethrin	CHAC, resorcinol, dopamine	CV	LOD = 6.7×10^{-14} M	[76]
Glyphosate	CS	EIS, CV	LOD = 0.001 pg/ml	[77]
Glyphosate	Ppy	SWV	LOD = 1 pM	[78]
Malathion	Bisacrylamide, TMEDA, APS	EIS, CV, DPV	LOD = 0.06 pg.mL^{-1}	[79]
Methyl parathion	MAA (FM), EGDMA (CL), AIBN (In)	-	LOD = 1.22×10^{-6} mg.L^{-1}	[80]
Methyl parathion	quercetin, resorcinol	CV	LOD = 0.01 μM	[81]
Methyl parathion	Zinc porphyrin, EGDMA (CL), AIBN (In)	DPV	LOD = 31,6 nM	[82]
Phosalone	-	SWV	LOD = 0.078 nM	[83]
Profenofos	SiO_2-	-	LOD = 2 nM	[84]

	vinylcarboxylat		S = 0.573 A.M^{-1}	
Imidacloprid	VBA, EGDMA (CL)	LSV	LOD = 0.10 μM	[85]
Mancozeb	IA (FN), EGDMA (CL)	SWV	LOD = 0.96 mg.L^{-1} DR = 5.96 – 257 mg.L^{-1}	[86]
Pirimiphos-methyl	CS-PVA, Gl, PMO	-	LOD = 0.2 nm	[87]
Methyl parathion	Phloroglucinol, NF	DPV	LOD = 1.5 ×10^{-13} g.mL^{-1} DR = 5 ×10^{-13} to 1.0 × 10^{-8} g.mL^{-1}	[88]
paraoxon	Phloroglucinol, NF	DPV	LOD = 3.4 × 10^{-14} g.mL^{-1} DR = 1.0 ×10^{-13} to 1.0 ×10^{-9} g.mL^{-1}	[88]
Catechol	Thienopyrrole, PFTBDT, Gl	-	LOD = 1.23 μM S = 737.4 μA.mM^{-1}.cm^{-2} DR = 1.25 to 175 μM	[89]
Paraoxon	PPy, CS	DPV	LOD = 0.17 nM	[90]
Acephate	PPy, aniline	CA	LOD = 0.007 ppm	[91]
Paraoxon	TTBO, Gl	-	LOD = 0.212 μM S = 8.076 μA μM^{-1} cm^{-2}	[92]
Malathion	PTT	CV	LOD = 4.08 nM S = 183.19 μA/mM	[93]
Atrazine	NH$_2$-BDC, PANI	-	LOD = 0.01 nM	[94]
Carbaryl	p-PD, IL	DPV	LOD = 0.09 mmol.L^{-1}	[95]

FM = functional monomer, CL = cross-linker, In = initiator, CV = Cyclic voltammetry, EIS = electrochemical impedance spectroscopy, DPV = Differential pulse voltammetry, CA = Chronoamperometry, SWV = Squarewave voltammetry, NF = Nafion, CS = chitosan, MPS = 3-mercaptopropyl)-trimethoxysilane, GdM = gadolinium molybdate (Gd_2MoO_6), CMCS = Carboxymethyl chitosan, MMA = methyl methacrylate, EGDMA = ethylene glycol dimethacrylate, AIBN = 2,2′ azobis(2-methylpropronitrile), CHAC = activated carbon prepared from coconut husk, TMEDA = N, N, N, N-tetramethyl ethylenediamine, APS = ammonium persulfate, MAA = methacrylic acid, VBA = p-vinylbenzoic acid, IA = itaconic acid, PVA = polyvinyl alcohol, PMO = pirimiphos- methyl oxon, Gl = glutaraldehyde, polypyrrole , PFTBDT = 1-(5-(4,8-bis(5-(2-ethylhexyl)thiophen-2-yl)benzo[1,2-b:4,5-b']dithiophen-2-yl)furan-2-yl)-5-(2-ethylhexyl)-3-(furan-2-yl)-4H thieno[3,4-c]pyrrole-4,6(5H)-dione, , PTT = [2,2 ;5′ 2″]-terthiophene-3-carbaldehyde, TTBO = 5,6-bis(octyloxy)-4,7-di(thieno[3][3,2-b]thiophen-2-yl)benzo[c][1,2,5]oxoadiazole, NH$_2$-BDC = 2-amino terephthalic acid, PANI = polyaniline, p-PD = p-Phenylenediamine, IL = ionic liquid.

5.2. Ion imprinted polymers

5.2.1. Ion imprinted vinylic polymers (IIVPs)

Organic imprinted polymers are synthesized mostly via free radical polymerization. Basically, vinyl groups are an appropriate category of polymerizable materials for such aim [10]. These polymerizable chelators are known as bifunctional agents; they possess a functionality according to their complexing capability [96]. Moreover, their activity extends to their vinyl function [9]. Crosslinking is an important point either in the presence of one or more functional monomer bearing a ligand [97] or a non-polymerizable ligand such as terpyridine among others [98, 99] or with linear chain polymers. This step has been classified into various mechanisms

[96]. It comprises crosslinking of linear polymers loaded with metal-binding groups (for example vinyl pyridine), beside chemical immobilization of commercially [100] or non-commercially available vinylated chelators that may interact with metal ions (see Figure 15 [101]).

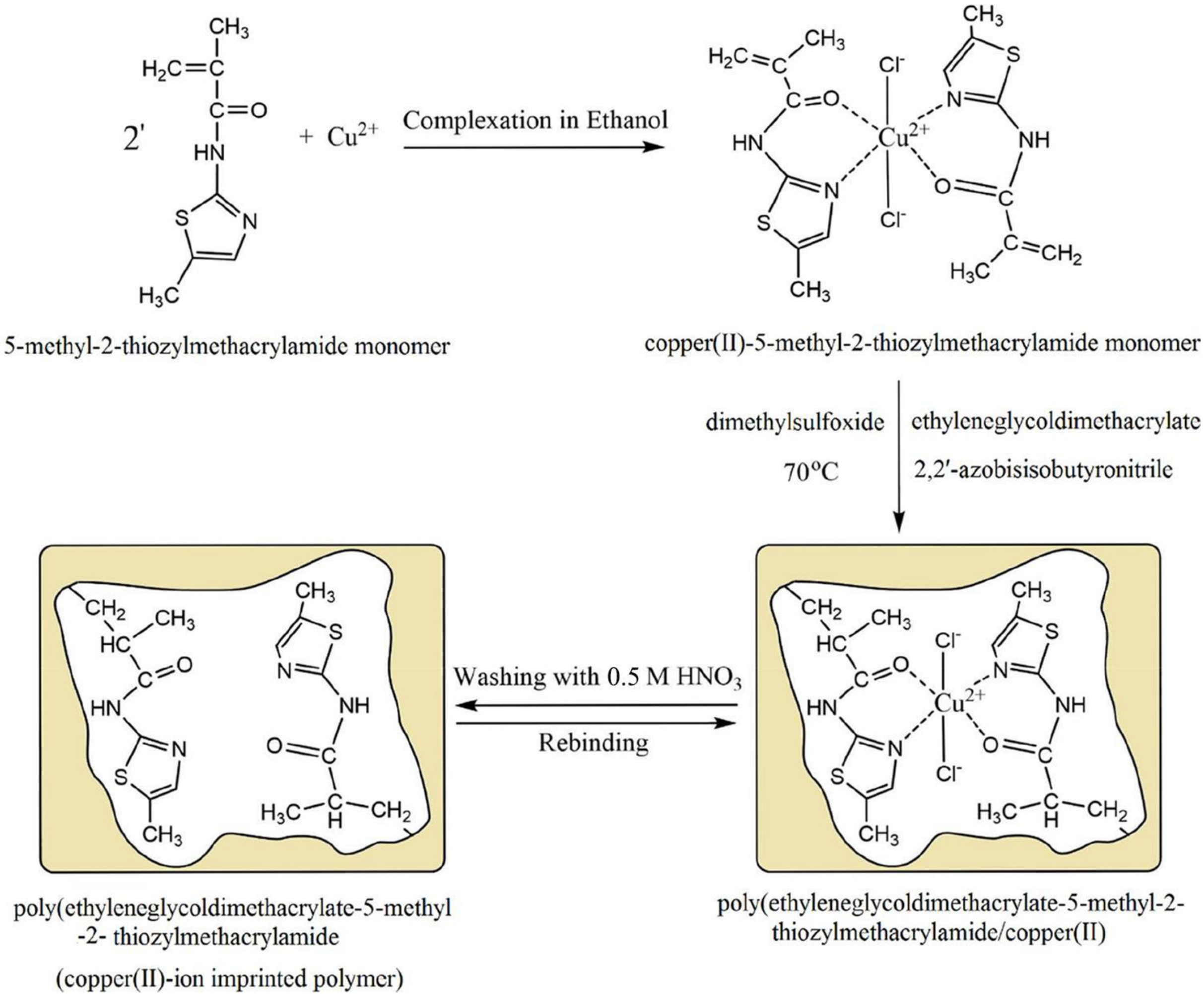

Figure 15. Schematic diagram for the preparation of the copper(II)-ion-imprinted polymer. The acrylamide derivative bearing thiozyl group serves as monomer and ligand in the same time. Adapted from [101].

Besides the choice of monomers, free or vinylated ligands, nanostructuration is also important. For example, multiwalled carbon nanotubes (MWCNTs) were used to make MWCNT-IIP nanocomposites for CPEs [102] or dispersed over SPE prior to IIP coating via surface-confined radical photopolymerization [103]. 4-fold higher response was obtained for SPE-CNT-IIVP sensor of Eu(III) compared to SPE-IIVP, that is the same system but without any MWCNTs (Figure 16). In this work, surface-confined UV-triggered photopolymerization was conducted with AIBN (Type I photoinitiator) and was found to provide electrochemical sensor with superior performances [103].

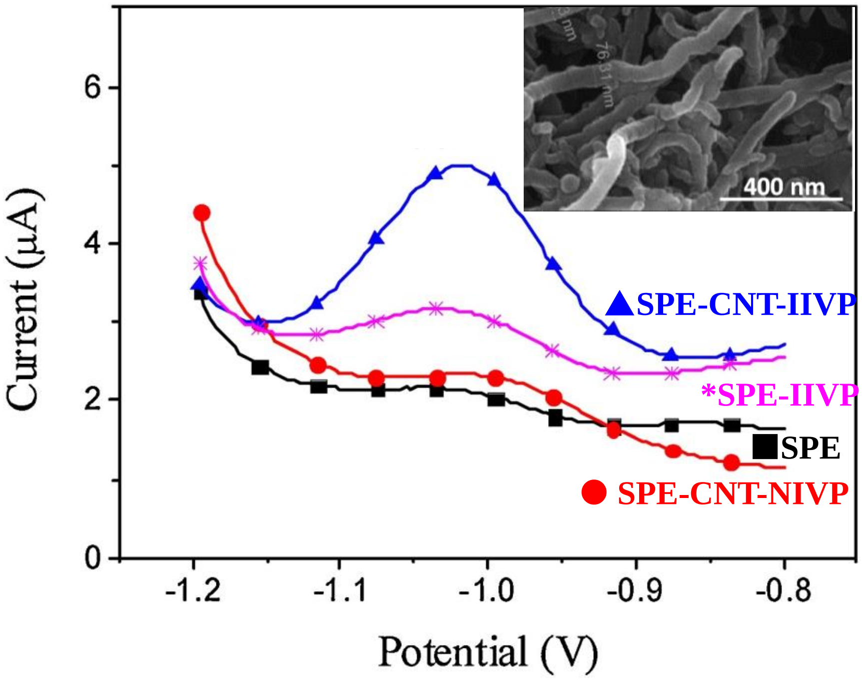

Figure 16. DPV output of 3.0×10^{-5} mol L^{-1} Eu^{3+} on bare and differently coated SPE electrodes at pH4.7. Adapted from [103].

In another study, a complex ion imprinted nanocomposite was designed based on both MWCNTs and halloysite nanotubes where the latter were grafted with hyperbranched IIP and the former ensured electron transfer to GCE [104].

5.2.2. Ion imprinted conductive polymers (IICPs)

Electrically conductive polymers are ideal for electrochemical applications because they do not require nanostructuration with carbon or metal to impart conductivity, and could be directly prepared on electrode surfaces within seconds to few minutes. They could also be prepared by precipitation oxidative polymerization in less than 2 h at RT, particularly polypyrrole. However, despite their physicochemical properties, they are only seldom applied for making imprinted polymer-based electrochemical sensors for the selective detection of metal ions. Recently, some of us summarized the findings on polypyrrole-based electrochemical sensors including ion imprinted polypyrroles [58]. Herein, we concentrate on the recent progress in the domain of ion imprinted conductive polymers, mainly polypyrrole, polyaniline and poly(phenylene diamine).

Before we summarize the recent progress on ion imprinted conductive polymers (IICPs), we would like to stress again that contrary to vinylic polymers, CPs have rigid structure and crosslinkers are quasi never employed. Despite the remarkable progress in the domain of imprinted polymers, little information is available on ion imprinted conjugated polymers for for electroanalysis of heavy metal ions. Handpicked examples of IICPs are reported in Table 5 reporting recent attractive studies with one decade old case of imprinted EDTA-like PPy.

In their quest of exploring PPy/EDTA-like type of sensors, the teams of Rivas and Moutet published a joint paper on IIPPy/EDTA-like for the selective detection of Hg^{2+}, Pb^{2+}, Cd^{2+} and Cu^{2+} (Figure 17). The strategy they devised permitted to achieve selective sensing and binding of Cd(II) in competitive mixtures containing other metal ions [105].

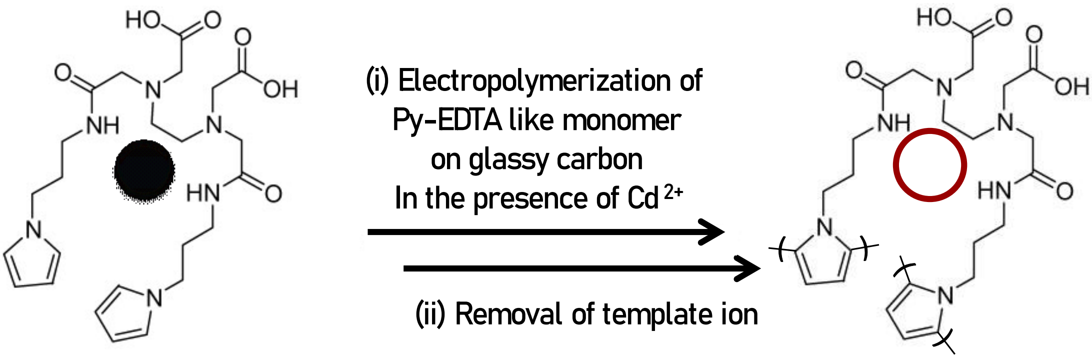

Figure 17. Strategy of preparation of an ion imprinted poly(pyrrole-EDTA like) polymer for the detection of Cd^{2+}. Step (i): preparation of the metallopolymer by electropolymerization of pyrrole-EDTA like/metal ion complex; step (ii): removal of the template ion and generation of artificial receptor sites within the polymer matrix. Adapted from [105].

Ion imprinting could be conducted with chelating co-dopants like L-cystein and acrylic acid as reported by some of us [106]. Herein, one explores the combined actions of chelating dopants and ion imprinting to achieve outstanding LOD for lead. In another strategy, Ait-Touchente et al. [107] reported 1 pM LOD, the lowest value ever reported for the detection of Hg^{2+}. In this work, they designed an IIP by electropolymerization of pyrrole in the presence of Hg^{2+} on ZnO nanorods that were grown on diazonium-modified gold electrodes (Figure 18).

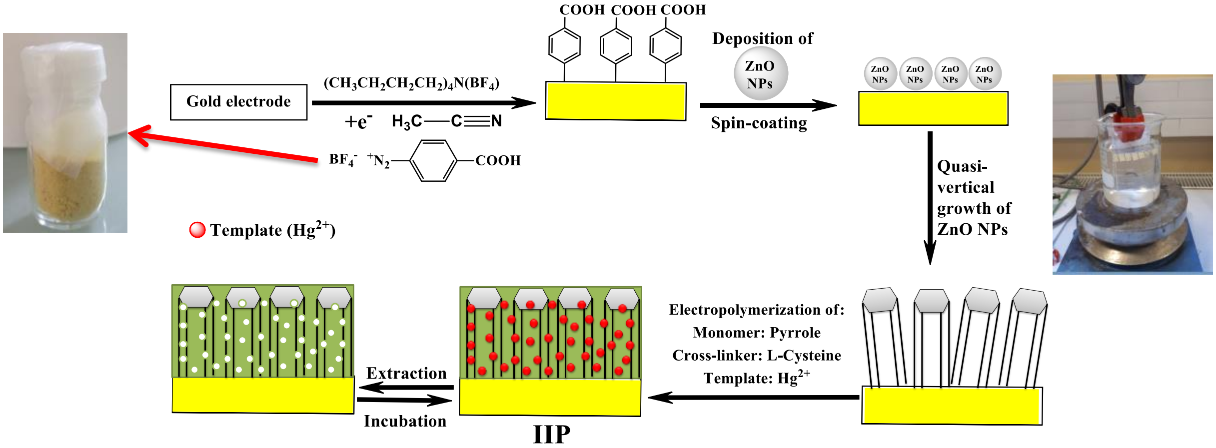

Figure 18. Schmatic illustration of the stepwise synthesis of mercury imprinted PPy wrapped around vertically aligned ZnO nanorods attached to diazonium-modified gold electrodes. Reproduced from [107].

5.2.3. Ion imprinted sol-gels (IISGs)

The sol-gel polymerization mainly uses silane molecules as main component, resulting in a solution that can be processed into many forms of polymer such as gel, coating and particles, all suitably adapted for the fabrication of IIP based electrochemical sensors. A few processes have been shortlisted and summarized hereafter.

Detection of copper ions Cu^{2+}

Copper ions were detected using copper imprinted sol-gel [108] bearing N1-[3-(trimethoxysilyl)propyl]diethylenetriamine (TPDT), which has the property of complexing copper ions with its diethylenetriamine group. The first step of IIP synthesis was the synthesis of ligand-functionalized silane. After complexation of Cu(II) for 24 h, the gel was crosslinked at reflux and washed to leach the Cu(II). This resulted in a copper ion imprinted sol-gel material (Figure 19) that served for making carbon paste electrode to track Cu(II) in tap water. LOD and sensitivity depended on pre-concentration time, optimally set at 1800 s. If LOD remains in the sub-micromolar regime, it is interesting to note that this IISG did not require any crosslinker such as TEOS and the synthesized TPDT silane was sufficient to make a 3D imprinted network. Interference studies have been done with Fe^{2+}, Zn^{2+}, Pb^{2+} and Ni$^{2=}$. Another feature, was the selectivity of the IISG to copper vs Ni(II), Zn(II) and Pb(II).

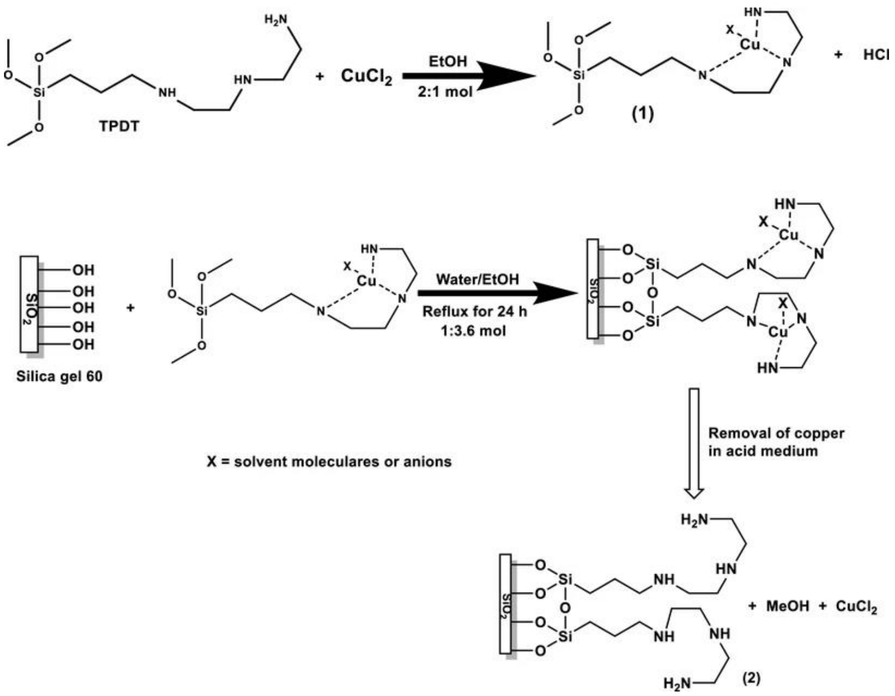

Figure 19. Synthesis of copper imprinted TPDT-functionalized silica. Reproduced from [108].

Detection of cadmium ions Cd^{2+}

In a similar study, carbon paste electrode has been prepared with cadmium imprinted sol-gel [109]. 3-[2-(2-aminoethylamino)ethylamino]propyl-tri methoxysilane (AAAPTS) has been used as the functional monomer, epichlorohydrin as cross-linker and Cd(II) ions as template; TEOS is used for the sol-gel process (Figure 20). The reaction of epichlorhydrin with NH groups opens the epoxy ring and yields OH groups which might enhance the hydrophilic character of the imprinted gel. After washing Cd^{2+} with HCl, the final IIP is in the form of fine powder. It was mixed with carbon into a paste. CPE was employed to track Cd(II) in a queous solutions prepared in lab, and in environmental water samples. The IISP had a LOD of 0,15 µg Cd.L^{-1}, the linear range was 0.5– 40 µg.L ^{1} and exhibited outstanding selectivity despite 30 to 100 fold more concentrated competitive metal ions. Indeed, no loss in recovery of Cd(II) was noted in the presence of other ions.

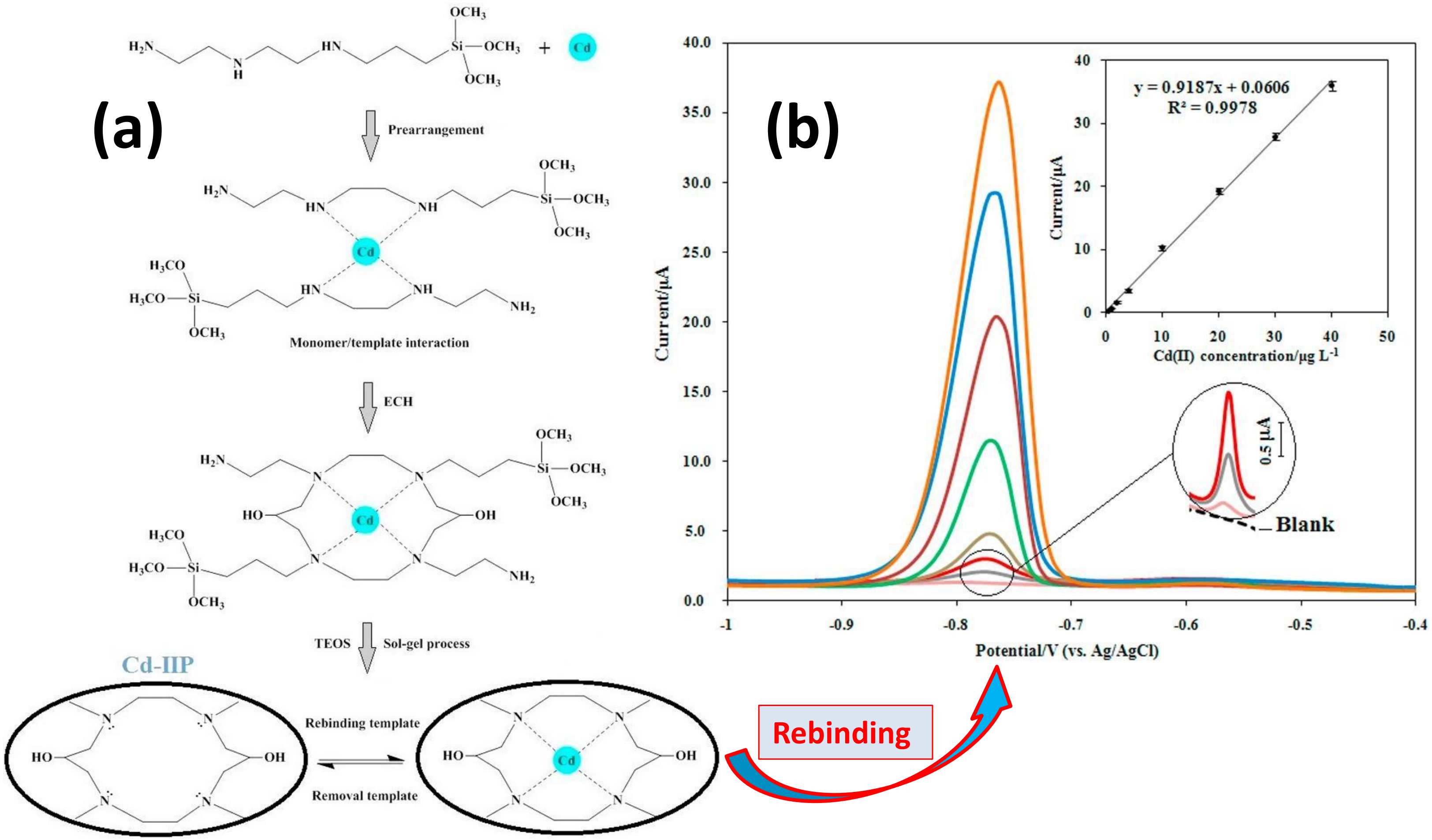

Figure 20. Synthesis of a cadmium ion imprinted sol-gel (a), and the use of its corresponding carbon paste for the highly sensitive detection of Cd(II). Reproduced from [109].

Detection of UO_2^{2+}

An interesting IISG has been proposed by Güney and Güney [110] with rarely employed 3-isocyanatopropyl trimethoxysilane (ICTMS) that was reacted with 3-aminoquinoline in order to obtain a functional silylated monomer bearing a quinolone ligand (Figure 21). The latter was crosslinked using tetramethylorthoxysilicate(TMOS) in the presence of UO_2(II). A CPE was made by mixing the UO_2(II)-imprinted sol-gel with carbon powder. The CPE exhibited a LOD of 3.07 × 10^{-10} mol.L^{-1}; the linear range was 2.0 × 10^{-9}–3.0 × 10^{-7} mol.L^{-1}. The sensor could be used to selectively detect uranyl in tap, pond and waste waters, with good recovery.

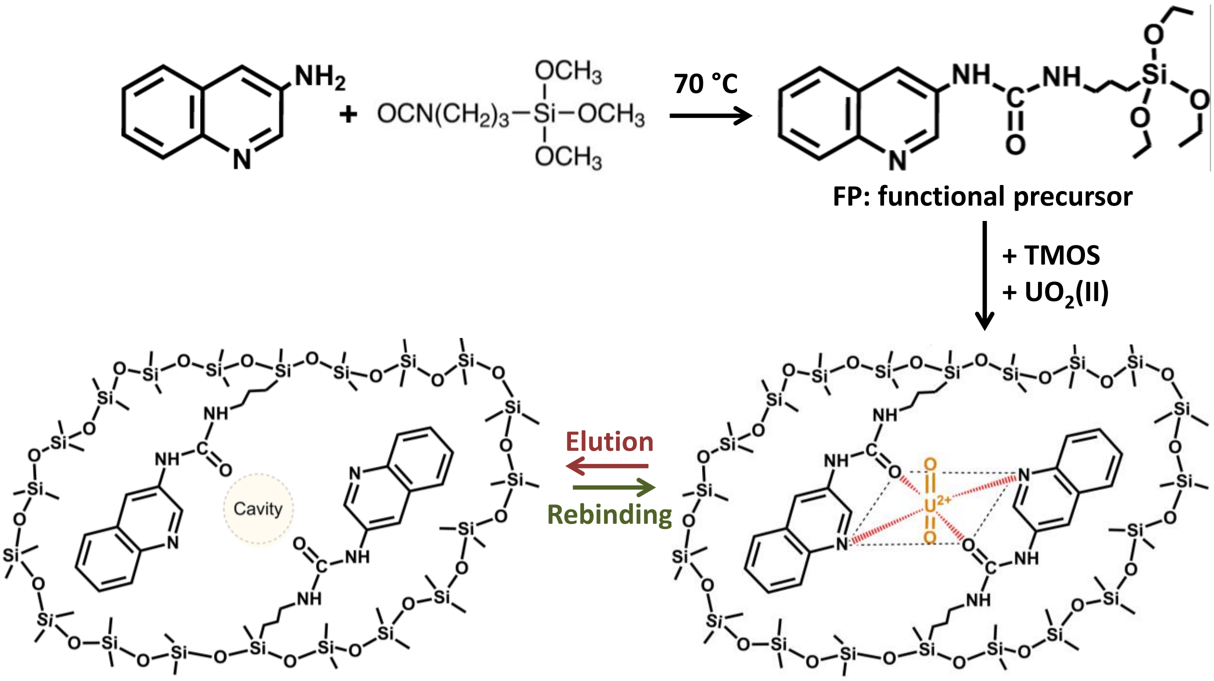

Figure 21. Synthesis of IISG from quinolone-functionalized silane, TMOS and uranyl. Adapted from [110].

Detection of europium Eu^{3+}

Europium is a reactive rare earth. The increasing applications of this element in the domain of industrial applications, material science, electronic engineering and life science raised toxilogy concerns, hence its traceability using IIPs [111].

The working electrode consisted of a screen sprinted electrode (SPE), coated with electrosynthesized polycatechol (PC), a signal amplifying element, and an IISG (Figure 22). The signal-amplifying element PC, bears hydroxyl groups and oxygen which could coordinate Eu^{3+} therefore improving the sensitivity and selectivity of Eu^{3+} IISG. The ion-imprinted sol-gel solution wass prepared using TEOS, PTMOS, MTMOS and Eu^{3+} solution. Note however that no reason was found to justify PTMOS and MTMOS silanes besides TEOS crosslinker.

The characterization of the fabricated electrode was performed by CV and EIS. Results show clear differences before and after Eu^{3+} removal: the current is weak and the resistance is strong before removal; after removal redox peak on CV was noted and the resistance decreased significantly. A clear difference between the IIP with and without PC has been observed: the peak current is nearly twice stronger for the IIP with PC, hence the effective signal amplifying property of PC.

DPASV has been used to determine the LOD and the linear range, they are respectively 1.0×10^{-7} mol.L^{-1} and 0.3 – 1000 µmol.L^{-1}. The sensor was found to be selective to Eu^{3+} over other metal ions. Indeed, peak current did not show any significant changes with the presence of competitive ions such as Ni^{2+}, Co^{2+}, Cu^{2+}, Fe^{3+} or Gd^{3+}.

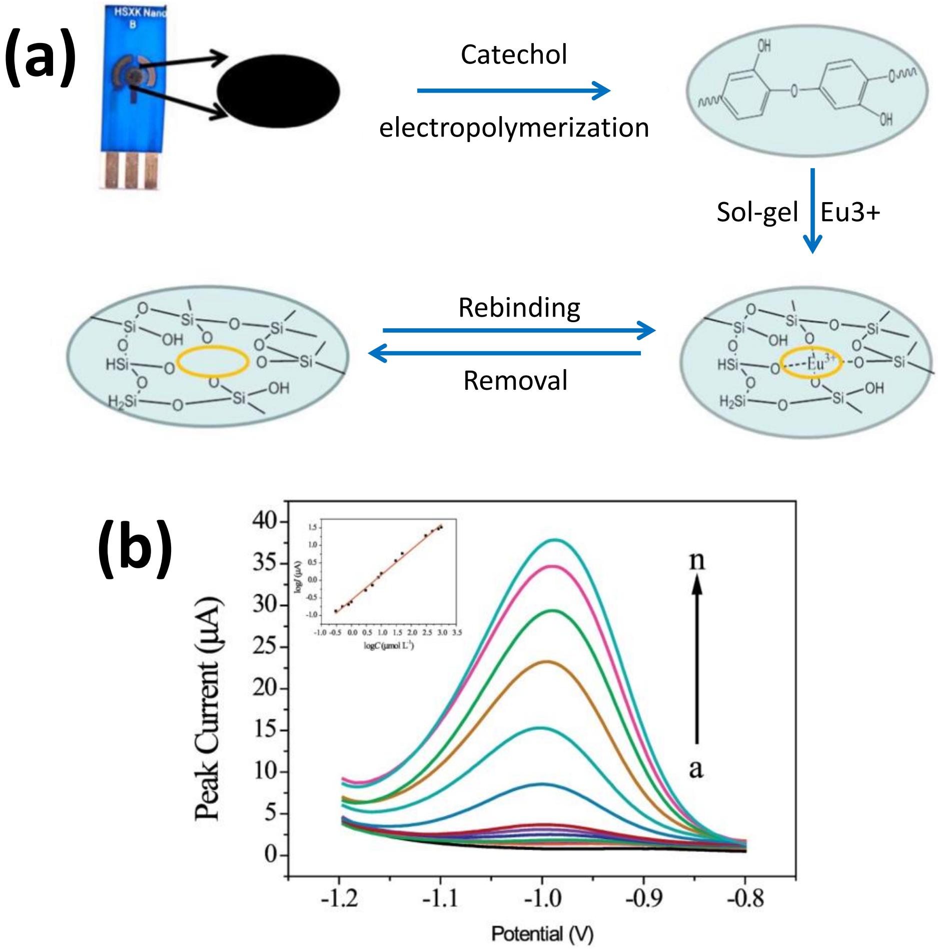

Figure 22. Two step preparation (a) and electrochemical Eu(III) sensing performance (b) of screen printed electrode coated with polycatechol-IISG bilayer.

The detection of Eu(III) was achieved by a bilayer of organic polymer that facilitates electron transfer and a sol-gel imprinted polymer that facilitates selective recognition. Recently, an ion imprinted hybrid polymer system (IIHP) has just been described, and consisted into imprinted, crosslinked vinylic polymer and sol-gel. –SH from MPS and imidazole group from the vinylic functional monomer have synergetic effect of Eu(III) complexation [112]. Each system (organic or sol-gel) had its own functional and crosslinker monomers (see Table 5) but 3-

(Trimethoxysilyl)propyl methacrylate served as coupling reagent for organic and inorganic phases. Indeed, it is a bifunctional molecule enabling to be involved in radical polymerization via the methacrylate end, and involved in sol-gel synthesis via the the trimethoxysilyl part. This sensor is certainly robust and highly selective, however, DPASV did not show any striking difference between the carbon paste electrode prepared from graphite powder only, and those prepared with IIHP and NIHP. The decreasing trend of the current intensity was CPE-IIHP(100 µA) > CPE-NIHP (80 µA) > CPE (55 µA).

5.2.4. Summary of experimental conditions of preparation and performances of ion imprinted polymers

Table 5 summarizes the experimental conditions for the synthesis of ion imprinted polymers as thin films or nanocomposites. Organic medium is required for vinylic polymers, whilst water/alcohol usually is considered for sol-gels. Conductive polymers require aqueous media, which is interesting in this respect, making the process “greener” and energy saving since the synthesis is usually conducted at RT. No clear trend concerning electrosensing; DPV and SWV seem to be randomly employed and return excellent LODs. From the shortlisted case studies, obviously CPEs are the most investigated and one should expect tremendeous development of CPEs in the near future.

Table 5. Design and performances of selected IIP electrodes.

Template/ Ligand/ Monomers/ Initiator	**Synthesis conditions**	**Final ion imprinted material**	**Detection technique**	**Performances**	**Year, Ref.**
Vinylic polymers					
Mn(II) / 1-(2-Pyridylazo)-2-naphthol / MAA & EGDMA/AIBN	Thermal radical polymerization at 60 °C, 24h; acid wash for 24 h then coating on MWCNT-Chit-IL-modified GCE	Mn(II)-IIP/MWCNT-Chit-IL coated on GCE	SWASV in acetate buffer, pH 6. 1.0 mg IIP, 2 min preconcentration at −1.4 V	LOD : 0.15 µM ; sensitivity 130.5 nA μM^{-1} cm^{-2}).	[113]
Pb(II) / 2,2′:6′,6″-terpyridine / EGDMA/AIBN	Thermal polymerization at 60 °C, 24h in DMF. 0.1 M HCl to remove Pb(II)	IIP-CPE-oil = 15/55/30%	DPASV in acetate buffer, pH 5. 6 min preconcentration at -1 V.	LOD: 0.11 nM; sensitivity 694 nA nM^{-1} cm^{-2}) for Pb(II) in the 0.4-10 nm range	[98]
Cu(II)/ 5-methyl-2-thiozylmethacrylamide/ EGDMA/AIBN	Thermal polymerization at 70 °C/12h then 80 °C/3h in DMSO. Cu(II) was removed in 0.5 M HNO_3.	Carbon paste: Cu(II) IIP 20%/65% C/5% MWCNTs/Parrafin oil 10%	Potentiometric titration of Cu(II) in EDTA at pH 6	Cu selective electrode. LOD $4.0{\times}10^{-7}$ M; stable at 4.0–8.0 pH range. Linear range: 1.0×10^{-6}–1.0×10^{-1} M Cu(II); Sensitivity: 26.1±0.9 mV/decade. Stable 1 year	[101]
Pb(II) / IA / EGDMA / AIBN	1 mmol $Pb(ClO_4)_2$ + 2 mmol IA in 35 mL CAN mixed for 30 min then 8 mmol EGDMA and 0.08 g AIBN added. Polymerization at 70 °C for 24h. Pb(II) leached using EDTA.	CPE: IIP/MWCNT/graphite/oil = 7/6/74.8/12.2 % w/w.	SWV in −0.7 to −0.2 V vs calomel; and scan rate = 500 mVs^{-1}, pH 5, preconcentration at -1V for 60 s.	LOD = 3.8 pmol L^{-1} ; Linear range = 1.0×10^{-11}–8.0×10^{-8} mol L^{-1}	[100]
Eu(III) / AM / EGDMA / AIBN	0.0125 mmol of $EuCl_3$ in 30 µL methanol+ 0.05 mmol AM in 0.47 mL + sonication + 30 dwell time + addition of 0.5 mmol EGDMA and 0.04 mmol AIBN. 1.5 µL of solution dropped on MWCNT-coated SPE. UV-triggered photopolyerization for 3h.	1.5 µL of template in monomer and AIBN solution was dropped on MWCNT-coated SPE. UV-triggered photopolyerization for 3h. Eu(III) removed in 0.6 M HCl at -1V vs Ag/AgCl.	DPV: −1.2 V to −0.6 V vs Ag/AgCl at pH 4.7; scan rate = 100 mV s^{-1}; see reference for details. Response of the sensor using $3.0{\times}10^{-5}$ mol L^{-1} Eu(III) is ~’ times higher for SPE/MWCNT-IIVP compared to SPE-IIVP.	LOD = 4.0×10−8 mol L^{-1}; linear range = $1.0{\times}10^{-7}$–$1.0{\times}10^{-3}$ mol L^{-1}. 95% of original response 30 uses or 2 month storage in water. Change in response less than 5% in the presence of 30-200 fold excess metal ions.	[103]
Conjugated polymers					
Hg^{2+}, Pb^{2+} Cd^{2+} Cu^{2+}/pyrrole-EDTA like	Oxidative electropolymerization in CH_3CN + TBAP	Film/CD	SWV	Hg^{2+}: LR=510^{-8} to 5.10^{-6}, LOD=10^{-7} ; $Pb^{2+:}$ -10^{-8} to 10^{-6}, LOD=5.10^{-10} ;	[105]

				Cd^{2+} : 10^{-7} to 10^{-5} LOD=510^{-7} ; Cu^{2+} : 510^{-8} to 2.510^{-7} LOD=5.10^{-9}	
Hg^{2+}/CMC/pyrrole	electropolymerization aqueous solution in KCL	Film/GCE	SWASV	20–800 µg$L^{-1.}$ LOD= 0.1µg.L^{-1}	[114]
Hg^{2+}/ pyrrole	Aqueous medium + NaCl Chronoamperometry performed on diazonium-modified gold electrode decorated with ZnO nanorods	IIPPy@ZnO NRs film coated on Au	SWASV	Sensitivity : 7.17 ± 0.15 µA/M; LOD : 10^{-12} M	[115]
Pb^{2+}/L-Cys/AA/pyrrole	Electropolymerization by CA on SAW sensor gold electrode. Conditions: 0.9 V/SCE, in water, pyrrole:10^{-2} M, L-Cys or AA: 10^{-4} M, Pb^{2+}: 10^{-3} M, LiClO4: 0.1 M.	Sensing imprinted L-Cys/PPy or AA/PPy	SWASV	LOD in the picomolar regime. [Pb^{2+}] detected in Bousselem river= 14 µg/l.	[106]
Cu^{2+} / para-phenylene diamine	CV in H_2SO_4 0.5M, 10mM of Cu^{2+} and 5 mM pPD on SPPtEs; 50 mV/s for 40 cycles.	Thin copper ion imprinted poly(para-phenylene diamine) films on SPPtED	DPV in the – 0.2 V to + 0.6 V range, in acetate buffer pH 5.2,	LOD: 2.7×10-9 ; LR= 9.0×10^{-10} – 1.5×10^{-8}, sensitivity= 1.30 µA nM^{-1}	[116]
Sol-gel polymers					
Cu(II) / TPDT	Complexation of Cu(II) by ligand-functionalized silane in ethanol followed by condensation of the silanols at reflux for 24h in water/ethanol.	Carbon paste of diethylenetriamine-functionalized copper ion-imprinted silica gel.	DPSAV at pH 5.2, in the -0.8 to +0.8 V potential range, pre-concentration time= 1800 s at Ered = –0.51 V vs SCE; scan rate = 20 mV s^{-1}.	LOD = 1.82×10^{-7} mmol L^{-1}. No significant change in sensor response in the presence of Fe(II), Ni(II), Zn(II) or Pb(II).The	[108]
Cd(II) / AAAPTS / ECH / TEOS	1 mmol of AAAPTS and 0.5 mmol $CdCl_2$ mixed in 100 mL anhydrous ethanol, 1h stirring and heating. Then 1 mmol of ECH added and stirring at 60 °C was conducted for 2 h. Finally 5 mmol TEOS and 2.5 mL NH4OH (14%) were added to the mixture under stirring and reactionleft to proceed for 12h.Sol-gel material was washed with ethanol than in 30 mL HCl (1 mol/L) to remove Cd(II).	CPE: graphite powder (57–75% (w/w)), IISG (0–13% (w/ w)) and paraffin oil (25% (w/w))	DPASV in the -1 to -0.4 V at pH 5, after 300 s accumulation in Cd(II) solution at -1.1 V vs Ag/AgCl,	10% IISG in CPE, LOD= LOD is 0,15 µg.L^{-1}, selective to Cd(II) in the presence of 30-100 fold excess competitive metal ions	[109]
Eu(III) / PTMOS / MTMOS/ TEOS / HCl in ethanol	Mixture of 50 µL TEOS, 50 µL ethanol, 30 µL PTMOS, 28 µL of MTMOS, 10 µL of 1×10^{-4} mol L^{-1} HCl and 50 µL of water left for 2h. deionized. 10 µL of 10 mmol L–1 Eu3+	SPE-polycatechol-IISG membrane.	DPV in buffer (pH 4.7) Eu(III): 3×10^{-7} to 10^{-3} M; accumulation at -0.2 V for 300 s; scan range: −1.2 to −0.6 V vs Ag/AgCl; scan	LOD = 1.0×10^{-7} mol.L^{-1}; linear range = 0.3 – 1000 µmol.L^{-1}; selectivity over Ni^{2+}, Co^{2+}, Cu^{2+}, Fe^{3+} or Gd^{3+} with 50-100 fold excess concentration.	[111]

	added to 90 µL of this mixture to obtain PPC. 1.5 µL of PCC solution dropped on SPE-polycatechol and left to gelify. IISG washing with HCl to remove Eu(III) template.		rate= 100 mV s^{-1}; amplitude=0.05 V.	Application to tap water, Greenlake water and Panlong river water.	
Cd(II) / **[**MPS / TMSPMA / TEOS**]** / **[**VIN / TRIM / AIBN**]**	0.18 g of Cd(NO$_3$)$_2$4H$_2$O in 10 mL of ethanol+ 0.90 mL VIN+1 mL MPS, 1.2 mL TMSPMA+ 1.1 mL TRIM+0.075 g AIBN. 10 min purge in N$_2$, then addition of 2 mL TEOS dissolved in ethanol and 0.95 mL of NaOH pH(1 molL^{-1}). Polymerization: 60 °C for 24 h in absence of oxygen. Template removed with HNO3 (1 molL^{-1}).	CPE- ion-imprinted hybrid polymer (IIHP). 80mg of graphite+20 mg IIHP+ 1mL of 0.1M KCl. After 12h drying, 85 µL mineral oil was added to obtain a compact paste.	Accumulation: 2000 µg/L^{-1} of Cd(II) at pH 1, -1.2 V vs. Ag/AgCl, for 300 s. DPASV in the -1 to -0.6 V in HCl 0.1 molL^{-1}.	Linear ranges: Cd(II) in the 1 to 100 µg.L^{-1} and 2.75-5.0 mgL^{-1}. LOD=0.10 µg.L^{-1}. Recovery > 93.6% in rivers and drinking water (Peru and Brazil). No interference with other metal ions, except for Hg(II) at 50 fold excess.	[112]
UO$_2$(II) / QFS / TMOS	Pre-gel: 40 mmol TMOS + 12 mL of propanol + 0.4 mL of 0.02 M HCl refluxed at 70 °C for 3 h. Sol: TMOS/QFS mixture. 0.1 ml of 0.1 M TEA added to catalyse sol-gel synthesis for 48h at RT and 24h at 100 °C. Final imprinted powder was crushed.	CPE preparation: carbon powder (CP) + IISG + paraffin oil (55:15:30) (% w/w).	DPCSV in the -0.4 - +0.4 V vs Ag/AgCl; accumulation time= 5min.	LOD = 3.07 × 10^{-10} mol.L^{-1}; linear range = 2.0 × 10^{-9}–3.0 × 10^{-7} mol.L^{-1}. No competitive effect of other metal ions. Application in tap, pond and waste waters.	[110]

AAAPTS : 3-[2-(2-aminoethylamino)ethylamino]propyl-tri methoxysilane; AA: acrylic acid; AM: acrylamide; CAN: acetonitrile; CD: carbon disk; CMC: Carboxy Methyl Cellulose; ECH: epichlorhydrin; FCN: K$_3$Fe(CN)$_6$, IA = itaconic acid; L-Cys: L-cystein; LR : linear range ; MR: Methyl Red; MTMOS : methyltrimethoxysilane ; NRs: nanorods; PPy-EDTA like: poly(N,N -ethylenebis[N-[(3-(pyrrole-1-yl)propyl) carbamoyl) methyl]- glycine ; pPD : p-phenylenediamine ; PQC: platinum quartz crystal; PTMOS : Phenyltrimethoxysilane ; SPPtEs : Platinum screen printed electrodes ; TBAP: Tetra-n-butylammonium perchlorate ; TMOS : Tetramethylorthosilicate ; TMSPMA : 3-(Trimethoxysilyl)propyl methacrylate ; TPDT: N1-[3-(trimethoxysilyl)propyl]diethylenetriamine; VIN: 1-vinylimidazole.

5.3. Bacteria imprinted polymers

Pathogens are infectious microorganisms, harmful to man. This section will emphasize waterborne pathogens. There are several ways to prepare MIP-based electrochemical sensors based on whole cell imprinting, surface imprinting, bacterial protein imprinting, quorum signaling molecules, spores or molecules that reflect the activity of the bacteria. The various approaches will be discussed through handpicked case studies.

5.3.1. Whole cell imprinting

Escherichia coli (*E. coli*) is rod shaped bacteria, it is normally harmless to human and we can generally find them in the intestines of livings. However, a few varieties can cause diseases such as abdominal cramps, bloody diarrhea and vomiting. These can be found in contaminated water or food. Jafari *et al.* [117] proposed an electrochemical sensor in which the sensing layer is a polymer layer synthetized by sol-gel methods, bacteria are added to the fresh sol solution at the end. Tetraethoxysilane (TEOS) has been used as the monomer for the polymerization, there is no need for a crosslinker here because this monomer acts as also a crosslinking agent. The electrochemical measurement is done by EIS with the following parameters: amplitude of 10mV at open circuit potential with a frequency range of 100 kHz-0.1 Hz. The result shows good selectivity when tests with *E. coli* and *S. aureus* (a spherical bacteria) has been conducted: when the sensor captures the corresponding bacteria, the charge transfer resistance increases, in the case of *S. aureus* the change of signal is greatly reduced. The same is true for *Pseudomonas aeruginosa*, another rod shaped bacterium. The performance of impedimetric sensor for *E.coli* is lower than other impedimetric sensor using *anti-E. coli* antibodies, but it has a low cost of preparation and a great limit of detection. The author has chosen the whole cell imprinting technique. This raises the issue of bacteria extraction from the *in situ* synthesized MIP film; as one can see in Figure 23, the washing of imprinted bacteria seems to seriously damage the imprinted sites. And as the author suggests more test with different bacteria should be done in order test the selectivity.

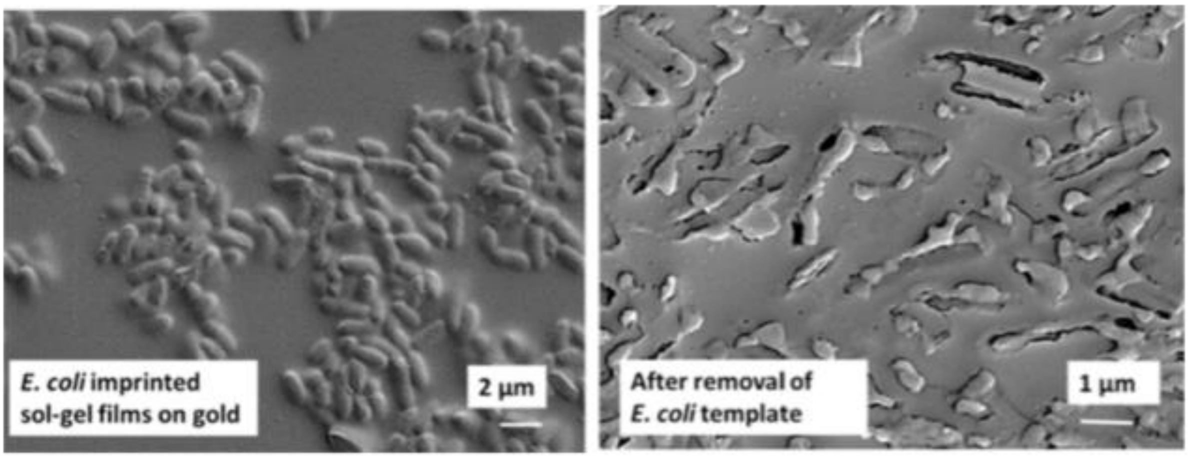

Figure 23 : SEM images of E.coli imprinting before (a) and after removal (b) of templates. Reproduced from [117].

5.3.2. *Bacterial surface imprinting*

As noted from SEM picture above (Figure 23(b)), imprinting of whole bacteria is not well adapted because of the size the template, however the imprinting of the surface or of a portion of bacteria is possible and better option (Figure 24). Sulfate reducing bacteria (SRB) are anaerobic microorganisms naturally presents in environmental sources such as soil, sea or river. They obtain their energy by reducing sulfate to sulfite, which is a highly corrosive and toxic substance. An electrochemical sensor for this type of bacteria has been fabricated by Qi *et al.* [53]. The monomer chosen for the film was chitosan (CS). CS becomes insoluble if the pH of the solution is higher than 6.3, in order to depose this monomer a potential is applied on the cathode in order to reduce H^+ to H_2, thus making the pH reach the threshold. SRB are deposed on the surface of the polymer film at the end, only a part of the surface of SRB is imprinted. However, the washing of bacteria after imprinting is difficult as it can make the recognition site larger or deform it. The impedimetric measurements show a really good selectivity when concentrations of other bacteria have been used (*S. aureus*, *M. luteus*, *V. alginolyticus*, *V. anguillarum*) as demonstrated in Figure 25.

Figure 25 shows Niquist plots for bioimprinted ITO before and after attachment of several bacteria (Figure 25A). As the receptor sites were shaped by SRB, this bacterium is recognized most. The Nyquist plot, for bioemprinted ITO with adsorbed SRB, shows the largest semi-circle on the Z' axis. The difference between Z' values for ITO, with and without bacteria, indicates resistance to charge transfer (ΔR_{ct}). It is the largest value for SRB because the sensor is indeed selective towards this bacterium (Figure 25B))..

This type of sensor is based on the size and shape of the bacteria, but the recognition site is fragile, a study on its reusability would be interesting, as one knows that biological bio-recognition elements, for example antibodies, can easily be damaged.

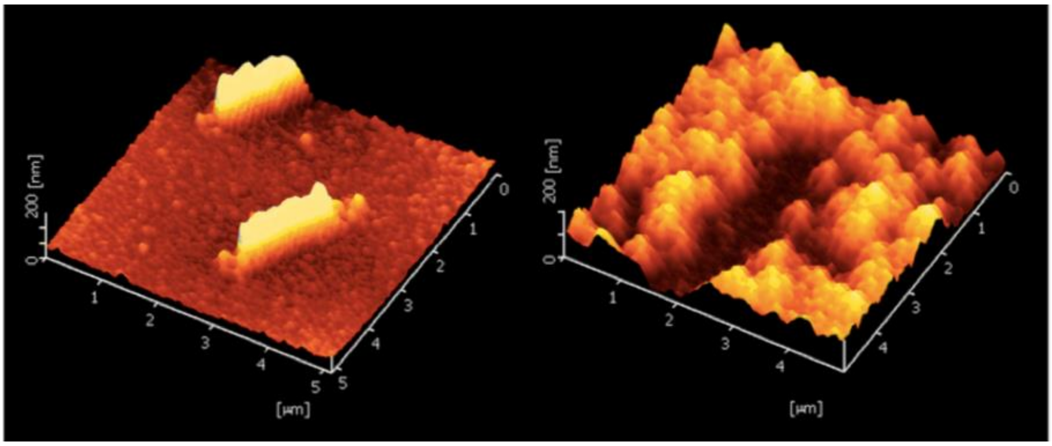

Figure 24. AFM image of bacteria imprinted polymer, before (felt) and after (right) washing

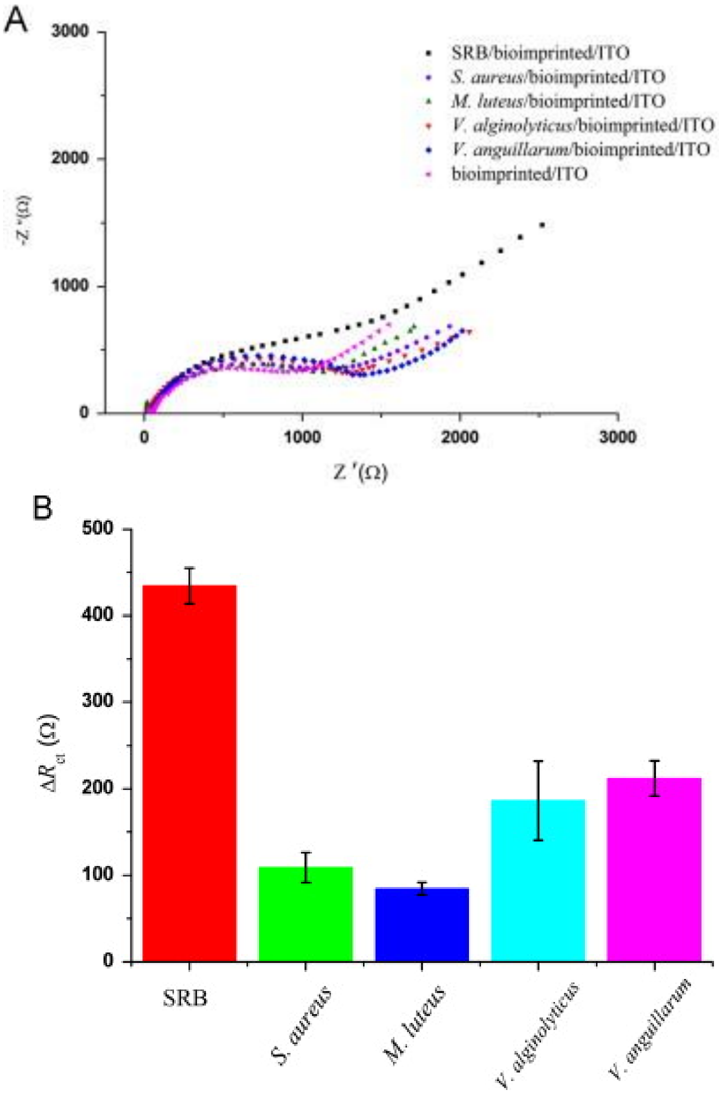

Figure 25. : Impedance spectra obtained with bioimprinted sensor and the biosensor after incubation with 1.0_10^8 cfu mL_1 SRB, S. aureus, M. luteus, V. anguillarum, and V. alginolyticus in PBS containing 5mM [Fe(CN)6]$^{4\_/3\_}$ as the probe(A).The comparison of Rct changes of the impedimetric biosensor based on SRB-mediated bioimprinted film to SRB, S. aureus, M. luteus, V. anguillarum, and V. alginolyticus (B). DRct is the change of charge transfer resistance of impedimetric sensor before and after incubation with different bacteria**.** Reproduced from [53].

5.3.3. *Bacterial protein A surface imprinting*

Imprinting a part of the surface of a pathogen is more efficient than imprinting a whole cellule, however the target is still too massive to enable recognition by functional groups. This disadvantage can be bypassed if the target is not the whole bacterium, but molecules and proteins specific to the said bacterium, for example specific surface protein. In a recent publication on electrochemical detection of Staphylococcus aureus (*S. aureus*), *Khan et al.* chose a representative protein (protein A) of the bacterium's outer surface as its target molecule [118]. Electropolymerization is done by CV on a film of single walled carbon nanotube (SWNCT) on which a solution of protein A has been deposited. Protein A (P) is a biological molecule, its washing can be achieved by using enzyme proteinase K which naturally degrade PA. The fabricated sensor shows good sensitivity when EIS test with PA and bovine serum albumin (BSA) has been done, however test with surface protein from other bacteria would give more argument to the efficacy of the sensor in selectively recognizing *S. aureus*.

5.3.4. *Imprinting of bacterial flagella proteins*

Another strategy is to detect proteins that act as specific flagella of bacteria. This approach is adopted by Khan *et al.* [119] for the detection of *Proteus mirabilis*. This bacterium can infect respiratory tract, urinary tract and open wounds, causing fever and pain. Its flagella are its mean to move in biological environment; moreover they are a mean to identify the bacteria as they are specific to them. The author chose phenol as monomer and achieved electropolymerization using CV (range from -0,2V to 0,8V; scan rate 50mV/s; 15 cycles). The methods of detection are EIS and SWV, results show excellent response in each method: for EIS, the impedance increases the more the sensing layer capture target molecules. For SWV, the pic current decreases when the concentration of flagella increases (Figure 26A). However, no such changes in the sensor response were noted with the non-imprinted polymer (Figure 26B) The selectivity is also good when the captor is used for a mixture of flagella/BSA and flagella/PA, the percentage of deviation in the response caused by interference is small for EIS(<8%) and SVW(<5%). The use of 2 method of electrochemical detection enables a better control of the quality of the sensor, and a selection of the most suitable method is done.

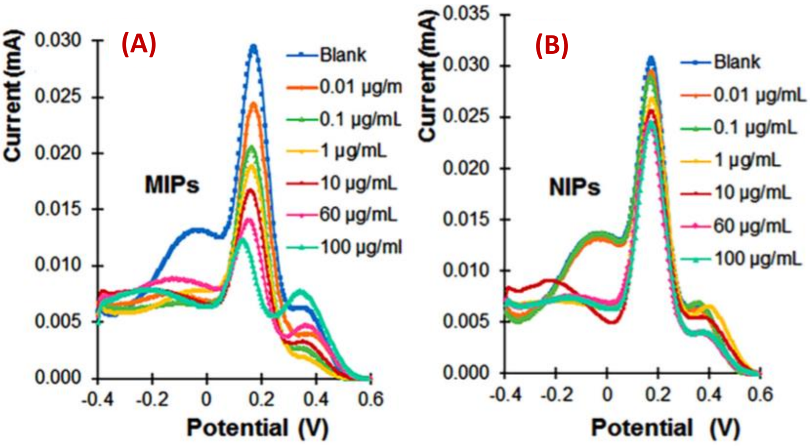

Figure 26. SWV voltammogram : result for MIP with different concentration of flagella (A, left) and result for NIP (B, right). Reproduced from [119].

5.3.5. *Bacterial spore imprinting*

Flagella are not the only specific protein one can detect from bacteria; spores released by them are also a mean to identify them. A bacterium releases spores when it is under stress, they are a mean of transmission: they develop into bacteria when ingested by animals or man. An approach of spore detection has been made by Ait Lahcen *et al.* [120], the objective is to detect specific spore released by Bacillus cereus and thus indirectly measure the quantity of this bacteria. Pyrrole has been chosen as a conductive monomer for cyclic voltammetry tests. The method of polymerization is still electropolymerization, however there is a small variation: the bacteria are introduced not at the beginning of polymerization, they are deposed in the middle of electropolymerization (5 cycles of CV, introduction of spores then 5 more cycles). This method shows more potential, when we compare the cyclic voltammogram of CPE/SIP when the spores are added at the beginning and the voltammogram when the spores are added at the middle of polymerization, the second one has better form than the first one, thus analysis with the chosen method of polymerization are more precise. The measurement is not direct; the sensor is first incubated 5 minutes in the selected concentration of *B. cereus* before measurement in order to bind the spores. The binding is also tested in a solution of 5 mM ferri/ferrocyanide in 0,1M KCl. Finally, after CV, the sensor shows good response and selectivity when another bacterium, B. subtilis, was mixed in the testing solution.

5.3.6. *Imprinting quorum sensing signaling molecules*

For the detection of the bacterium Aeromonas hydrophila, Jiang *et al.* [121] chose another surface protein as the target: N-acryl-homoserine-lactones (AHLs) are molecules that can induce the expression of pathogenic factors. They intervene in the quorum sensing system (QS), a system that enables bacteria to communicate between them and play a key role in determining virulence (Figure 27).

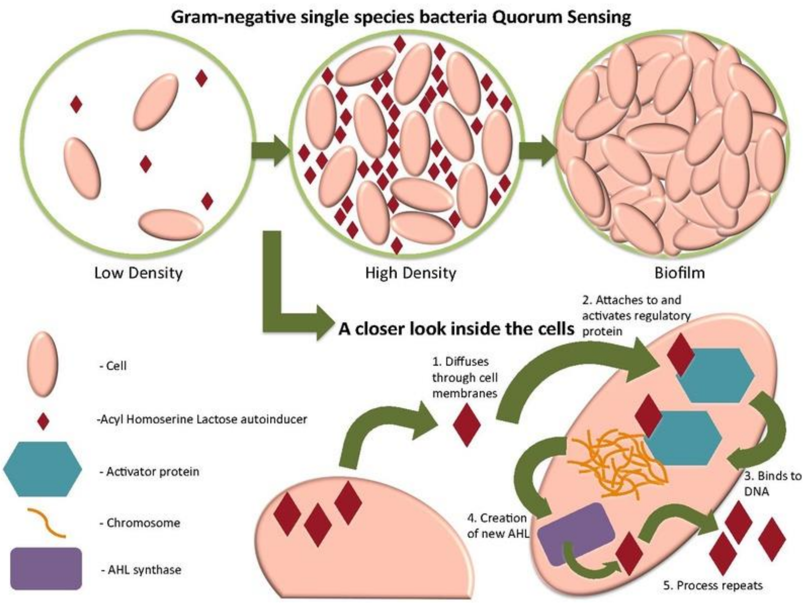

Figure 27 : Mechanisms of quorum sensing from isolated bacteria to the formation of biofilms. Early detection of quorum sensing signaling molecules will require action to prevent biofilm formation. Reproduced from [121].

AHL is generally produced at a low concentration, it is thus difficult to detect. MIP can solve this problem owing to the combined high selectivity of MIPs and outstanding sensitivity of electrochemical devices. In this publication magnetic molecularly imprinted polymer (MMIP) are used as the sensing element. First Fe_3O_4 magnetic nanoparticles are prepared using a solvothermal method, after that silica-shell deposition is done with tetraethyl orthosilicate (TEOS), then introduction of amine groups with 3-Methacryloxypropyltrimethoxylane (APTES), finally polymerization will be done in the surface of these magnetic nanoparticle with an analogue template proteins (DMHF) ; in the end one obtains polymerized nanoparticles. The detection of AHLs is done as follow: first MMIP is incubated in a solution of target proteins, after 4 minutes magnetic glassy carbon electrode (MGCE), the working electrode, is introduced in the solution and the MMIP will attach magnetically to the electrode. When all detection sites of MMIP are occupied, the electron-transfer resistance between the heart of MMIP and the electrode is maximal. This resistance decreases when captured proteins are washed off from MMIP.

The chosen detection method is DPV; results show that the selectivity of the MMIP is good when tests with DMHF in the presence of structural analogues of AHLs including C4-AHL, C6-AHL, C8-AHL and N-3oxo-C6-HSL have been conducted. The stability of the electrochemical sensor seems to be right: a test has been conducted with MMIP stored for about three months; no particular changes have been noted. Finally, the detection range of AHLs is from 2.5×10^{-9} mol.L^{-1} to 1.0×10^{-7} mol.L^{-1}.

5.3.7. Summary of bacteria imprinted polymers

Table 6 summarizes shortlisted case studies tackled in this mini-review. It concerns the bacterium under test, the monomer employed to make the MIP, the electrode material, the polymerization technique, the electrochemical technique and the limit of detection (LOD). Despite the low number of entries, Table 6 testifies for the rich literature on bacterial sensing using MIP-based electrodes and particularly the numerous strategies for recognizing bacteria without necessarily going through the problematic whole cell imprinting technique.

To finish, care must be taken when designing these MIP-based electrochemical sensors as reproducibility is an issue. It takes time and several trials/errors to obtain a system that is validated by various labs. This should be done in an inter-laboratory experience to test a given type of bacterial electrochemical sensors.

The recovery should not be a concern; and clearly one could note development of low-cost disposable electrodes. Probably in this sense, the development of highly selective and sensitive paper electrodes will avoid the problem of contamination by hazardous compounds as they can be disposed of by simple burning [122].

Table 6. Synoptic table reporting shortlisted MIP-based electrochemical sensors for the detection of a range of bacteria. The MIPs were prepared using bacteria or their specific molecular or macromolecular compounds.

Target	Functional monomer	Electrode Material	Polymerization technique	Detection method	LOD	Ref.
E. Coli	TEOS	Gold	Sol-gel imprinting	EIS	1 cfu /mL	[117]
S. Aureus	AP	Carbon	Electropolymerization	CV, EIS	0,60nM	[118]
Aeromas hydrophila (AHLs)	MAA, DMHF	Magnetic Glassy carbon	Controlled Radical polymerization	DPV	8.10^{-10} mol/L	[121]
Bacillus cereus (spore)	Pyrrole	Carbon paste	Electropolymerization	CV	10^2cfu/mL	[120]
Proteus mirabilis (flagella)	Phenol	Carbon	Electropolymerization	CV, EIS, SWV	0.9 ng/mL	[119]
Sulfate-reducing bacteria	CS	ITO/graphene	Electrodeposition	EIS	$0.7.10^4$ cfu/mL	[53]

AP : 3-aminophenol; CS: Chitosan; DMHF : 2,5-dimethyl-4-hydroxy-3(2H)-furanone ; MAA : Methacrylic acid

Conclusion

In this review, we have summarized the recent developments of imprinted polymer-based electrochemical sensors (focus on 2017-2021). We have considered vinylic, conjugated and sol-gel type polymers. We targeted pesticides, heavy metal ions and bacteria as templates for the making of imprinted organic and inorganic polymers. From the synoptic tables, thermally induced radical polymerization is time consuming and requires 24h; surface-confined photopolymerization is faster. Sol-gel polymerization requires one day to complete, but polymerization of conjugated polymers is probably the most time-saving technique, particularly when it is electrochemically triggered (a few minutes suffices). As far as performances are concerned, electrochemistry is an excellent technique to achieve outstanding limits of detection, in the nanomolar or even better in the picomolar regime. Improvements are certainly brought by new technologies enabling to record signals with high S/N ratios, at extremely low concentrations of analytes. We also discussed the interest of nanostructuration with carbon nanotubes or graphene, but also hybrid filling consisting in nanostructuration with both MWCNTs and clay nanotubes. If direct coating of the imprinted polymers on the electrodes remains very established method, the design of separate nanocomposites prior to their deposition on flat glassy carbon electrodes or their mixture with graphite powder to make carbon paste electrodes seems irreversibly approved. Indeed, we witness more and more research studies on imprinted polymer nanocomposites coated on GCE and protected by Nafion or in the form of CPEs.

Achievement of very high performances is tedious, and hundreds of inspiring strategies are offered to the specialist or the new comer in the field. Protocols should, however, be tested and adapted to the context of the study and to the targeted pollutant be it organic/inorganic compound or pathogenic micro-organism.

To sum up, the prevailing design of MIP sensors in the last decade has attempted to demonstrate high performances depending on theoretical and functional models. However, in spite of these positive results, more attention is required to improve the MIP sensors synthesis technologies in order to use them in real samples and environment monitoring of pollutants. The MIP-based electrochemical sensors can be considered as alternatives for existing patented and industrialized devices, which permits to pave the way for large scale commercial use and reach high technology readiness level [33]. In this sense, molecular imprinting remains a very interesting and commercially viable technology that will possibly be competitive within the diagnostic market for the next coming years [123].

Acknowledgements

AMK wishes to thank the French Embassy in Egypt (Institut Francais d'Egypte) and Science and Technology Developing Fund (STDF)-Egypt for the provision of a fellowship (Project No 42248).

The authors declare no conflict of interest

Author Contributions:

Conceptualization of the research work by X.Z., M.M.C.and N.F.

Methodology by X.Z., M.M.C.and N.F.

Validation by M.M.C., N.F.

Writing of Original Draft was done by X.Z., M.M.C., S.K.

Writing: Review and Editing: All co-authors

Supervision, M.M.C. and N.F.

Funding Acquisition, A.M.K., M.M.C.

References

1. Kümmerer, K., et al., *A path to clean water.* Science, 2018. **361**(6399): p. 222-224.
2. Stradiotto, N.R., H. Yamanaka, and M.V.B. Zanoni, *Electrochemical sensors: a powerful tool in analytical chemistry.* Journal of the Brazilian Chemical Society, 2003. **14**(2): p. 159-173.
3. Zhou, A.Y., et al., *A portable bioelectronic sensing system (BESSY) for environmental deployment incorporating differential microbial sensing in miniaturized reactors.* PloS one, 2017. **12**(9): p. e0184994.
4. Saylan, Y., et al., *Molecularly imprinted polymer based sensors for medical applications.* Sensors, 2019. **19**(6): p. 1279.
5. Cao, Y., et al., *Recent advances of molecularly imprinted polymer-based sensors in the detection of food safety hazard factors.* Biosensors and Bioelectronics, 2019. **141**: p. 111447.
6. Arreguin-Campos, R., et al., *Imprinted Polymers as Synthetic Receptors in Sensors for Food Safety.* Biosensors, 2021. **11**(2): p. 46.
7. Waheed, A., M. Mansha, and N. Ullah, *Nanomaterials-based electrochemical detection of heavy metals in water: current status, challenges and future direction.* TrAC Trends in Analytical Chemistry, 2018. **105**: p. 37-51.
8. Beluomini, M.A., et al., *Electrochemical sensors based on molecularly imprinted polymer on nanostructured carbon materials: A review.* Journal of Electroanalytical Chemistry, 2019. **840**: p. 343-366.
9. Branger, C., W. Meouche, and A. Margaillan, *Recent advances on ion-imprinted polymers.* Reactive and Functional Polymers, 2013. **73**(6): p. 859-875.

10. Hande, P.E., A.B. Samui, and P.S. Kulkarni, *Highly selective monitoring of metals by using ion-imprinted polymers.* Environmental Science and Pollution Research, 2015. **22**(10): p. 7375-7404.
11. Adumitrăchioaie, A., et al., *Electrochemical methods based on molecularly imprinted polymers for drug detection. A review.* Int. J. Electrochem. Sci, 2018. **13**: p. 2556-2576.
12. Lahcen, A.A. and A. Amine, *Recent advances in electrochemical sensors based on molecularly imprinted polymers and nanomaterials.* Electroanalysis, 2019. **31**(2): p. 188-201.
13. Mahmoudpour, M., et al., *Nanomaterial-based molecularly imprinted polymers for pesticides detection: Recent trends and future prospects.* TrAC Trends in Analytical Chemistry, 2020: p. 115943.
14. Karrat, A., et al., *Applications of Chitosan in Molecularly and Ion Imprinted Polymers.* Chemistry Africa, 2020: p. 1-21.
15. Negm, N.A., et al., *Advancement on modification of chitosan biopolymer and its potential applications.* International journal of biological macromolecules, 2020. **152**: p. 681-702.
16. Wei, P., et al., *Fe3O4/SiO2/CS surface ion-imprinted polymer modified glassy carbon electrode for highly sensitivity and selectivity detection of toxic metal ions.* Journal of the Taiwan Institute of Chemical Engineers, 2020. **113**: p. 107-113.
17. Cheong, W.J., S.H. Yang, and F. Ali, *Molecular imprinted polymers for separation science: a review of reviews.* Journal of separation science, 2013. **36**(3): p. 609-628.
18. Ndunda, E.N., *Molecularly imprinted polymers—A closer look at the control polymer used in determining the imprinting effect: A mini review.* Journal of Molecular Recognition, 2020. **33**(11): p. e2855.
19. Li, L., et al., *Molecularly imprinted polymers for extraction of malachite green from fish samples prior to its determination by HPLC.* Microchimica Acta, 2015. **182**(9): p. 1791-1796.
20. Piletsky, S.A. and A.P. Turner, *Electrochemical sensors based on molecularly imprinted polymers.* Electroanalysis: An International Journal Devoted to Fundamental and Practical Aspects of Electroanalysis, 2002. **14**(5): p. 317-323.
21. Suryanarayanan, V., C.T. Wu, and K.C. Ho, *Molecularly imprinted electrochemical sensors.* Electroanalysis, 2010. **22**(16): p. 1795-1811.
22. Naarmann, H., *Strategies for synthesizing conducting polymers.* Synthetic metals, 1991. **41**(1-2): p. 1-6.
23. Ansari, R., *Polypyrrole conducting electroactive polymers: synthesis and stability studies.* E-Journal of Chemistry, 2006. **3**(4): p. 186-201.
24. Dickey, F.H., *The preparation of specific adsorbents.* Proceedings of the National Academy of Sciences of the United States of America, 1949. **35**(5): p. 227.
25. Wuff, G. and A. Sarhan, *The use of polymers with enzyme-analogous structures for the resolution of racemate.* Angew. Chem. Int. Ed, 1972. **11**: p. 341-345.
26. Boitard, C., et al., *Whole Protein Imprinting over Magnetic Nanoparticles Using Photopolymerization.* ACS Applied Polymer Materials, 2019. **1**(5): p. 928-932.
27. Ahmad, R., et al., *Water-soluble plasmonic nanosensors with synthetic receptors for label-free detection of folic acid.* Chemical Communications, 2015. **51**(47): p. 9678-9681.

28. Msaadi, R., et al., *Highly selective copper ion imprinted clay/polymer nanocomposites prepared by visible light initiated radical photopolymerization.* Polymers, 2019. **11**(2): p. 286.
29. Msaadi, R., et al., *Diazonium-based ion-imprinted polymer/clay nanocomposite for the selective extraction of lead (II) ions in aqueous media.* European Polymer Journal, 2017. **89**: p. 367-380.
30. Bakas, I., et al., *Molecularly imprinted polymeric sensings layers grafted from aryl diazonium‐modified surfaces for electroanalytical applications. A mini review.* Surface and Interface Analysis, 2014. **46**(10-11): p. 1014-1020.
31. Mousli, F., et al., *Surface Modification of Polymeric Substrates with Photo‐and Sonochemically Designed Macromolecular Grafts.* Surface Modification of Polymers: Methods and Applications, 2019: p. 273-315.
32. Ahmad, R., et al., *Nanocomposites of gold nanoparticles@ molecularly imprinted polymers: chemistry, processing, and applications in sensors.* Chemistry of Materials, 2015. **27**(16): p. 5464-5478.
33. Ahmad, O.S., et al., *Molecularly imprinted polymers in electrochemical and optical sensors.* Trends in biotechnology, 2019. **37**(3): p. 294-309.
34. Tajik, S., et al., *Recent developments in conducting polymers: applications for electrochemistry.* RSC Advances, 2020. **10**(62): p. 37834-37856.
35. Choi, W., T. An, and G. Lim, *Fabrication of conducting polymer nanowires.* Nanowires-Implementations and Applications, 2011: p. 440-454.
36. Naveen, M.H., N.G. Gurudatt, and Y.-B. Shim, *Applications of conducting polymer composites to electrochemical sensors: A review.* Applied Materials Today, 2017. **9**: p. 419-433.
37. Kaur, G., A. Kaur, and H. Kaur, *Review on nanomaterials/conducting polymer based nanocomposites for the development of biosensors and electrochemical sensors.* Polymer-Plastics Technology and Materials, 2020: p. 1-18.
38. Nezakati, T., et al., *Conductive polymers: opportunities and challenges in biomedical applications.* Chemical reviews, 2018. **118**(14): p. 6766-6843.
39. Mandi, U., et al., *Chromium (VI) grafted mesoporous polyaniline as a reusable heterogeneous catalyst for oxidation reactions in aqueous medium.* RSC Advances, 2014. **4**(30): p. 15431-15440.
40. Peterson, D.S., *Sol–Gel Technique*, in *Encyclopedia of Microfluidics and Nanofluidics*, D. Li, Editor. 2013, Springer US: Boston, MA. p. 1-7.
41. Huang, J., et al., *Electrochemical sensor based on imprinted sol–gel and nanomaterials for sensitive determination of bisphenol A.* Food Control, 2011. **22**(5): p. 786-791.
42. Zhang, Z., et al., *Layer-by-layer assembly sensitive electrochemical sensor for selectively probing l-histidine based on molecular imprinting sol–gel at functionalized indium tin oxide electrode.* Biosensors and Bioelectronics, 2010. **26**(2): p. 696-702.
43. Ghanei-Motlagh, M. and M.A. Taher, *Novel imprinted polymeric nanoparticles prepared by sol–gel technique for electrochemical detection of toxic cadmium(II) ions.* Chemical Engineering Journal, 2017. **327**: p. 135-141.
44. McCreery, R.L., *Advanced carbon electrode materials for molecular electrochemistry.* Chemical reviews, 2008. **108**(7): p. 2646-2687.
45. Gam‐Derouich, S., et al., *Aryl diazonium salt surface chemistry and ATRP for the preparation of molecularly imprinted polymer grafts on gold substrates.* Surface and Interface Analysis, 2010. **42**(6‐7): p. 1050-1056.

46. Mahouche-Chergui, S., et al., *Aryl diazonium salts: a new class of coupling agents for bonding polymers, biomacromolecules and nanoparticles to surfaces.* Chemical Society Reviews, 2011. **40**(7): p. 4143-4166.
47. Matyjaszewski, K., et al., *Grafting from surfaces for "everyone": ARGET ATRP in the presence of air.* Langmuir, 2007. **23**(8): p. 4528-4531.
48. Zoppe, J.O., et al., *Surface-initiated controlled radical polymerization: state-of-the-art, opportunities, and challenges in surface and interface engineering with polymer brushes.* Chemical reviews, 2017. **117**(3): p. 1105-1318.
49. Xu, X., et al., *A novel molecularly imprinted sensor for selectively probing imipramine created on ITO electrodes modified by Au nanoparticles.* Talanta, 2009. **78**(1): p. 26-32.
50. Sulitzky, C., et al., *Grafting of molecularly imprinted polymer films on silica supports containing surface-bound free radical initiators.* Macromolecules, 2002. **35**(1): p. 79-91.
51. Bakas, I., et al., *Picomolar detection of melamine using molecularly imprinted polymer‐based electrochemical sensors prepared by UV‐graft photopolymerization.* Electroanalysis, 2015. **27**(2): p. 429-439.
52. Iskierko, Z., et al., *Molecularly imprinted polymers for separating and sensing of macromolecular compounds and microorganisms.* Biotechnology advances, 2016. **34**(1): p. 30-46.
53. Qi, P., Y. Wan, and D. Zhang, *Impedimetric biosensor based on cell-mediated bioimprinted films for bacterial detection.* Biosensors and Bioelectronics, 2013. **39**(1): p. 282-288.
54. Mazzotta, E., et al., *Solid-phase synthesis of electroactive nanoparticles of molecularly imprinted polymers. A novel platform for indirect electrochemical sensing applications.* Sensors and Actuators B: Chemical, 2016. **229**: p. 174-180.
55. Simões, F.R. and M.G. Xavier, *Electrochemical sensors.* Nanoscience and its Applications, 2017: p. 155-178.
56. Deroco, P.B., et al., *based electrochemical sensing devices*, in *Comprehensive Analytical Chemistry*. 2020, Elsevier. p. 91-137.
57. Brett, C. and A.M. Oliveira Brett, *Electrochemistry: principles, methods, and applications*. 1993.
58. Lo, M., et al., *Polypyrrole: a reactive and functional conductive polymer for the selective electrochemical detection of heavy metals in water.* Emergent Materials, 2020: p. 1-25.
59. Kanoun, O., *Impedance Spectroscopy: Advanced Applications: Battery Research, Bioimpedance, System Design*. 2019: De Gruyter.
60. Choi, W., et al., *Modeling and applications of electrochemical impedance spectroscopy (EIS) for lithium-ion batteries.* Journal of Electrochemical Science and Technology, 2020. **11**(1): p. 1-13.
61. Gupta, R., et al., *Advances in nanomaterial-based electrochemical biosensors for the detection of microbial toxins, pathogenic bacteria in food matrices.* Journal of Hazardous Materials, 2021. **401**: p. 123379.
62. Zhang, Z., J. Zhou, and X. Du, *Electrochemical biosensors for detection of foodborne pathogens.* Micromachines, 2019. **10**(4): p. 222.
63. Beduk, T., et al., *A paper-based inkjet-printed PEDOT:PSS/ZnO sol-gel hydrazine sensor.* Sensors and Actuators B: Chemical, 2020. **306**: p. 127539.

64. Arduini, F., et al., *Nanomaterials in electrochemical biosensors for pesticide detection: advances and challenges in food analysis.* Microchimica Acta, 2016. **183**(7): p. 2063-2083.
65. Chapalamadugu, S. and G.R. Chaudhry, *Microbiological and biotechnological aspects of metabolism of carbamates and organophosphates.* Critical reviews in biotechnology, 1992. **12**(5-6): p. 357-389.
66. Pundir, C. and A. Malik, *Bio-sensing of organophosphorus pesticides: a review.* Biosensors and Bioelectronics, 2019. **140**: p. 111348.
67. Hu, H., et al., *Acetylcholinesterase Sensor with Patterned Structure for Detecting Organophosphorus Pesticides Based on Titanium Dioxide Sol‐gel Carrier.* Electroanalysis, 2020.
68. Cui, H.-F., et al., *A highly stable acetylcholinesterase biosensor based on chitosan-TiO2-graphene nanocomposites for detection of organophosphate pesticides.* Biosensors and Bioelectronics, 2018. **99**: p. 223-229.
69. Zhang, J., et al., *An acetylcholinesterase biosensor with high stability and sensitivity based on silver nanowire–graphene–TiO 2 for the detection of organophosphate pesticides.* RSC advances, 2019. **9**(43): p. 25248-25256.
70. Song, Y., et al., *A simple electrochemical biosensor based on AuNPs/MPS/Au electrode sensing layer for monitoring carbamate pesticides in real samples.* Journal of Hazardous Materials, 2016. **304**: p. 103-109.
71. Maulidiyah, M., et al., *Sol-gel TiO2/Carbon Paste Electrode Nanocomposites for Electrochemical-assisted Sensing of Fipronil Pesticide.* Journal of Electrochemical Science and Technology, 2019. **10**(4): p. 394-401.
72. Vinoth Kumar, J., et al., *3D flower-like gadolinium molybdate catalyst for efficient detection and degradation of organophosphate pesticide (fenitrothion).* ACS applied materials & interfaces, 2018. **10**(18): p. 15652-15664.
73. Wei, X.-P., et al., *In-situ non-covalent dressing of multi-walled carbon nanotubes@ titanium dioxides with carboxymethyl chitosan nanocomposite electrochemical sensors for detection of pesticide residues.* Materials & Design, 2016. **111**: p. 445-452.
74. Aman, S., et al., *Cypermethrin toxicity: a review.* J. of Fors. Sci. and Cri. Inves, 2018. **9**(4): p. 555767.
75. Leepheng, P., et al., *An experimental and theoretical study of molecularly imprinted electrode based on methyl methacrylate polymer for pesticide detection.* Japanese Journal of Applied Physics, 2020. **59**(SI): p. SIIJ09.
76. Li, Y., et al., *A robust electrochemical sensing of molecularly imprinted polymer prepared by using bifunctional monomer and its application in detection of cypermethrin.* Biosensors and Bioelectronics, 2019. **127**: p. 207-214.
77. Zouaoui, F., et al., *Electrochemical impedance spectroscopy determination of glyphosate using a molecularly imprinted chitosan.* SENSORS AND ACTUATORS B-CHEMICAL, 2020. **309**.
78. Mazouz, Z., et al., *Highly selective polypyrrole MIP-based gravimetric and electrochemical sensors for picomolar detection of glyphosate.* Sensors, 2017. **17**(11): p. 2586.
79. Aghoutane, Y., et al., *Development of a molecularly imprinted polymer electrochemical sensor and its application for sensitive detection and determination of malathion in olive fruits and oils.* Bioelectrochemistry, 2020. **132**: p. 107404.

80. Hassan, A.H., et al., *Electrochemical sensing of methyl parathion on magnetic molecularly imprinted polymer.* Biosensors and Bioelectronics, 2018. **118**: p. 181-187.
81. Wang, F.-R., et al., *Electrochemical sensor using molecular imprinting polymerization modified electrodes to detect methyl parathion in environmental media.* Electrocatalysis, 2018. **9**(1): p. 1-9.
82. He, B., et al., *A porphyrin molecularly imprinted biomimetic electrochemical sensor based on gold nanoparticles and carboxyl graphene composite for the highly efficient detection of methyl parathion.* Nano, 2017. **12**(04): p. 1750046.
83. Xu, L., et al., *A disposable molecularly imprinted electrochemical sensor for the ultra-trace detection of the organophosphorus insecticide phosalone employing monodisperse Pt-doped UiO-66 for signal amplification.* Analyst, 2020. **145**(9): p. 3245-3256.
84. Amatatongchai, M., et al., *Novel three-Dimensional molecularly imprinted polymer-coated carbon nanotubes (3D-CNTs@MIP) for selective detection of profenofos in food.* Analytica Chimica Acta, 2019. **1076**: p. 64-72.
85. Zhang, M., et al., *Molecularly imprinted polymer on graphene surface for selective and sensitive electrochemical sensing imidacloprid.* Sensors and Actuators B: Chemical, 2017. **252**: p. 991-1002.
86. Kumar, S., et al., *Molecularly imprinted star polymer-modified superparamagnetic iron oxide nanoparticle for trace level sensing and separation of mancozeb.* RSC advances, 2016. **6**(43): p. 36751-36760.
87. El-Moghazy, A.Y., et al., *Biosensor based on electrospun blended chitosan-poly (vinyl alcohol) nanofibrous enzymatically sensitized membranes for pirimiphos-methyl detection in olive oil.* Talanta, 2016. **155**: p. 258-264.
88. Dong, S., et al., *Conducting microporous organic polymer with –OH functional groups: Special structure and multi-functional integrated property for organophosphorus biosensor.* Chemical Engineering Journal, 2021. **405**: p. 126682.
89. Yasa, M., et al., *Construction of amperometric biosensor modified with conducting polymer/carbon dots for the analysis of catechol.* Journal of Polymer Science, 2020. **58**(23): p. 3336-3348.
90. Akdag, A., M. Işık, and H. Göktaş, *Conducting polymer-based electrochemical biosensor for the detection of acetylthiocholine and pesticide via acetylcholinesterase.* Biotechnology and Applied Biochemistry, 2020. **n/a**(n/a).
91. Kondawar, S.B., et al., *Conductive polymer nanocomposite enzyme immobilized biosensor for pesticide detection.* Journal of Materials NanoScience, 2019. **6**(1): p. 7-12.
92. Turan, J., et al., *An effective surface design based on a conjugated polymer and silver nanowires for the detection of paraoxon in tap water and milk.* Sensors and Actuators B: Chemical, 2016. **228**: p. 278-286.
93. Guler, M., V. Turkoglu, and A. Kivrak, *Electrochemical detection of malathion pesticide using acetylcholinesterase biosensor based on glassy carbon electrode modified with conducting polymer film.* Environmental Science and Pollution Research, 2016. **23**(12): p. 12343-12351.
94. Bhardwaj, S.K., et al., *Immunosensing of Atrazine with Antibody-Functionalized Cu-MOF Conducting Thin Films.* ACS Applied Materials & Interfaces, 2015. **7**(47): p. 26124-26130.

95. Salih, F.E., et al., *Conducting Polymer/Ionic Liquid Composite Modified Carbon Paste Electrode for the Determination of Carbaryl in Real Samples.* Electroanalysis, 2018. **30**(8): p. 1855-1864.
96. Rao, T.P., R. Kala, and S. Daniel, *Metal ion-imprinted polymers—novel materials for selective recognition of inorganics.* Analytica Chimica Acta, 2006. **578**(2): p. 105-116.
97. Yolcu, M. and N. Dere, *A novel copper selective sensor based on ion imprinted 2-vinylpyridine polymer.* Canadian Journal of Chemistry, 2018. **96**(12): p. 1027-1036.
98. Shamsipur, M., et al., *Synthesis, characterization and using a new terpyridine moiety-based ion-imprinted polymer nanoparticle: sub-nanomolar detection of Pb (II) in biological and water samples.* Chemical Papers, 2018. **72**(11): p. 2707-2717.
99. Shamsipur, M., et al., *Development of an ultrasensitive electrochemical genosensor for detection of HIV-1 pol gene using a gold nanoparticles coated carbon paste electrode impregnated with lead ion-imprinted polymer nanomaterials as a novel electrochemical probe.* Microchemical Journal, 2021. **160**: p. 105714.
100. Alizadeh, T., et al., *An extraordinarily sensitive voltammetric sensor with picomolar detection limit for Pb2+ determination based on carbon paste electrode impregnated with nano-sized imprinted polymer and multi-walled carbon nanotubes.* Journal of environmental chemical engineering, 2017. **5**(5): p. 4327-4336.
101. Topcu, C., et al., *Electrochemical determination of copper (II) in water samples using a novel ion-selective electrode based on a graphite oxide–imprinted polymer composite.* Analytical Letters, 2018. **51**(12): p. 1890-1910.
102. Alizadeh, T., et al., *Development of a highly selective and sensitive electrochemical sensor for Bi3+ determination based on nano-structured bismuth-imprinted polymer modified carbon/carbon nanotube paste electrode.* Sensors and Actuators B: Chemical, 2017. **245**: p. 605-614.
103. Chen, J., et al., *Stripping voltammetric determination of europium via ultraviolet-trigger synthesis of ion imprinted membrane.* Sensors and Actuators B: Chemical, 2018. **271**: p. 329-335.
104. Ying-Lu, H., et al., *Preparation and Cadmium Ion Sensing Properties of Ionic Imprinted Materials Based on HNTs.* CHINESE JOURNAL OF INORGANIC CHEMISTRY, 2019. **35**(10): p. 1755-1766.
105. Pereira, E., et al. *Complexing polymer films in the preparation of modified electrodes for detection of metal ions*. in *Macromolecular Symposia*. 2011. Wiley Online Library.
106. Sakhraoui, H.E.E.Y., et al., *Design of L-cysteine and acrylic acid imprinted polypyrrole sensors for picomolar detection of lead ions in simple and real media.* IEEE Sensors Journal, 2019. **20**(8): p. 4147-4155.
107. Ait-Touchente, Z., et al., *High performance zinc oxide nanorod-doped ion imprinted polypyrrole for the selective electrosensing of mercury II ions.* Applied Sciences, 2020. **10**(19): p. 7010.
108. Villis, P.C.M., et al., *Diethylenetriamine ion-imprinted silica gel for copper determination in tap water.* Journal of Applied Electrochemistry, 2018. **48**(8): p. 867-883.

109. Ghanei-Motlagh, M. and M. Taher, *Novel imprinted polymeric nanoparticles prepared by sol–gel technique for electrochemical detection of toxic cadmium (II) ions.* Chemical Engineering Journal, 2017. **327**: p. 135-141.
110. Güney, S. and O. Güney, *A novel electrochemical sensor for selective determination of uranyl ion based on imprinted polymer sol–gel modified carbon paste electrode.* Sensors and Actuators B: Chemical, 2016. **231**: p. 45-53.
111. Chen, J., et al., *Electrochemical sensor for detection of europium based on poly-catechol and ion-imprinted sol-gel film modified screen-printed electrode.* Journal of Electroanalytical Chemistry, 2018. **824**: p. 32-38.
112. Adauto, A., et al., *A selective electrochemical sensor for the detection of Cd (II) based on a carbon paste electrode impregnated with a novel ion ‐ imprinted hybrid polymer.* Electroanalysis.
113. Roushani, M., et al., *Preparation an electrochemical sensor for detection of manganese (II) ions using glassy carbon electrode modified with multi walled carbon nanotube-chitosan-ionic liquid nanocomposite decorated with ion imprinted polymer.* Journal of Electroanalytical Chemistry, 2017. **804**: p. 1-6.
114. Velempini, T., et al., *Application of a polypyrrole/carboxy methyl cellulose ion imprinted polymer in the electrochemical detection of mercury in water.* Electroanalysis, 2018. **30**(11): p. 2612-2619.
115. Ait-Touchente, Z., et al. *Zinc oxide nanorods wrapped with ion-imprinted polypyrrole polymer for picomolar selective and electrochemical detection of mercury II ions*. in *Multidisciplinary Digital Publishing Institute Proceedings*. 2018.
116. Di Masi, S., et al., *Sensor based on electrosynthesised imprinted polymeric film for rapid and trace detection of copper (II) ions.* Sensors and Actuators B: Chemical, 2020. **307**: p. 127648.
117. Jafari, H., et al., *Entrapment of uropathogenic E. coli cells into ultra-thin sol-gel matrices on gold thin films: A low cost alternative for impedimetric bacteria sensing.* Biosensors and Bioelectronics, 2019. **124**: p. 161-166.
118. Khan, M.A.R., et al., *Plastic antibody for the electrochemical detection of bacterial surface proteins.* Sensors and Actuators B: Chemical, 2016. **233**: p. 697-704.
119. Khan, M.A.R., et al., *Artificial receptors for the electrochemical detection of bacterial flagellar filaments from Proteus mirabilis.* Sensors and Actuators B: Chemical, 2017. **244**: p. 732-741.
120. Lahcen, A.A., et al., *Label-free electrochemical sensor based on spore-imprinted polymer for Bacillus cereus spore detection.* Sensors and Actuators B: Chemical, 2018. **276**: p. 114-120.
121. Jiang, H., et al., *Magnetic molecularly imprinted polymer nanoparticles based electrochemical sensor for the measurement of Gram-negative bacterial quorum signaling molecules (N-acyl-homoserine-lactones).* Biosensors and Bioelectronics, 2016. **75**: p. 411-419.
122. Cho, J.H., Y. Gao, and S. Choi, *A portable, single-use, paper-based microbial fuel cell sensor for rapid, on-site water quality monitoring.* Sensors, 2019. **19**(24): p. 5452.
123. Lowdon, J.W., et al., *MIPs for commercial application in low-cost sensors and assays–An overview of the current status quo.* Sensors and Actuators B: Chemical, 2020: p. 128973.